World Journal of Biological Chemistry

Submit a Manuscript: http://www.wjgnet.com/esps/
Help Desk: http://www.wjgnet.com/esps/helpdesk.aspx
DOI: 10.4331/wjbc.v7.i1.188

World J Biol Chem 2016 February 26; 7(1): 188-205
ISSN 1949-8454 (online)

ORIGINAL ARTICLE

Basic Study

Epigenetic alteration to activate Bmp2-Smad signaling in Raf-induced senescence

Mai Fujimoto, Yasunobu Mano, Motonobu Anai, Shogo Yamamoto, Masaki Fukuyo, Hiroyuki Aburatani, Atsushi Kaneda

Mai Fujimoto, Shogo Yamamoto, Hiroyuki Aburatani, Atsushi Kaneda, Genome Science Division, Research Center for Advanced Science and Technology, the University of Tokyo, Tokyo 153-8904, Japan

Mai Fujimoto, Yasunobu Mano, Masaki Fukuyo, Atsushi Kaneda, Department of Molecular Oncology, Graduate School of Medicine, Chiba University, Chiba 260-8670, Japan

Motonobu Anai, Laboratory for Systems Biology and Medicine, Research Center for Advanced Science and Technology, the University of Tokyo, Tokyo 153-8904, Japan

Atsushi Kaneda, CREST, Japan Agency for Medical Research and Development, Tokyo 100-0004, Japan

Author contributions: Fujimoto M and Mano Y performed the majority of the experiments; Fujimoto M and Anai M participated in the treatment of animals; Fujimoto M, Mano Y, Yamamoto S and Fukuyo M analyzed the data; Aburatani H and Kaneda A designed and coordinated the research; Fujimoto M, Mano Y and Kaneda A wrote the paper.

Supported by The CREST program, Japan Agency for Medical Research and Development to Kaneda A, and grants from the Uehara Memorial Foundation, Takeda Science Foundation, and Public Trust Surgery Research Fund to Kaneda A.

Institutional review board statement: This study was reviewed and approved by Institutional Review Board of the University of Tokyo.

Institutional animal care and use committee statement: All of the procedures involving animals were reviewed and approved by Institutional Animal Care and Use Committee of the University of Tokyo (IACUC protocol number: RAC120108).

Conflict-of-interest statement: The authors have no conflict of interest.

Data sharing statement: A technical appendix and dataset are available from the corresponding author at kaneda@chiba-u.jp.

Correspondence to: Atsushi Kaneda, MD, PhD, Professor, Department of Molecular Oncology, Graduate School of Medicine, Chiba University, Inohana 1-8-1, Chuo-ku, Chiba 260-8670, Japan. kaneda@chiba-u.jp
Telephone: +81-43-2262039
Fax: +81-43-2262039

Received: June 26, 2015
Peer-review started: July 16, 2015
First decision: September 17, 2015
Revised: October 30, 2015
Accepted: December 3, 2015
Article in press: December 4, 2015
Published online: February 26, 2016

Abstract

AIM: To investigate epigenomic and gene expression alterations during cellular senescence induced by oncogenic *Raf*.

METHODS: Cellular senescence was induced into mouse embryonic fibroblasts (MEFs) by infecting retrovirus to express oncogenic *Raf* (RafV600E). RNA was collected from RafV600E cells as well as MEFs without infection and MEFs with mock infection, and a genome-wide gene expression analysis was performed using microarray. The epigenomic status for active H3K4me3 and repressive H3K27me3 histone marks was analyzed by chromatin

immunoprecipitation-sequencing for RafV600E cells on day 7 and for MEFs without infection. These data for *Raf*-induced senescence were compared with data for *Ras*-induced senescence that were obtained in our previous study. Gene knockdown and overexpression were done by retrovirus infection.

RESULTS: Although the expression of some genes including secreted factors was specifically altered in either *Ras*- or *Raf*-induced senescence, many genes showed similar alteration pattern in *Raf*- and *Ras*-induced senescence. A total of 841 commonly upregulated 841 genes and 573 commonly downregulated genes showed a significant enrichment of genes related to signal and secreted proteins, suggesting the importance of alterations in secreted factors. *Bmp2*, a secreted protein to activate Bmp2-Smad signaling, was highly upregulated with gain of H3K4me3 and loss of H3K27me3 during *Raf*-induced senescence, as previously detected in *Ras*-induced senescence, and the knockdown of *Bmp2* by shRNA lead to escape from *Raf*-induced senescence. Bmp2-Smad inhibitor *Smad6* was strongly repressed with H3K4me3 loss in *Raf*-induced senescence, as detected in *Ras*-induced senescence, and senescence was also bypassed by Smad6 induction in *Raf*-activated cells. Different from *Ras*-induced senescence, however, gain of H3K27me3 did not occur in the *Smad6* promoter region during *Raf*-induced senescence. When comparing genome-wide alteration between *Ras*- and *Raf*-induced senescence, genes showing loss of H3K27me3 during senescence significantly overlapped; genes showing H3K4me3 gain, or those showing H3K4me3 loss, also well-overlapped between *Ras*- and *Raf*-induced senescence. However, genes with gain of H3K27me3 overlapped significantly rarely, compared with those with H3K27me3 loss, with H3K4me3 gain, or with H3K4me3 loss.

CONCLUSION: Although epigenetic alterations are partly different, *Bmp2* upregulation and *Smad6* repression occur and contribute to *Raf*-induced senescence, as detected in *Ras*-induced senescence.

Key words: Senescence; Epigenome; *Raf*; H3K27me3; Histone; *Ras*

Core tip: By examining gene expressions and active and repressive histone marks on genome-wide scale, many genes were found to show common expression changes during *Ras*- and *Raf*-induced senescence, including genes related to secreted factors and cell cycle. Upregulation of *Bmp2* and downregulation of *Smad6* were detected and played a role in *Raf*-induced senescence as well as in *Ras*-induced senescence. Epigenetic alterations to regulate gene expression were also similar, including gain and loss of active histone mark H3K4me3 and loss of H3K27me3. But epigenetic changes are different in part, *e.g.*, in gain of H3K27me3 in *Smad6* promoter region.

Fujimoto M, Mano Y, Anai M, Yamamoto S, Fukuyo M, Aburatani H, Kaneda A. Epigenetic alteration to activate Bmp2-Smad signaling in Raf-induced senescence. *World J Biol Chem* 2016; 7(1): 188-205 Available from: URL: http://www.wjgnet.com/1949-8454/full/v7/i1/188.htm DOI: http://dx.doi.org/10.4331/wjbc.v7.i1.188

INTRODUCTION

Cellular senescence is a phenomenon of permanent growth arrest after the limited cell division of primary culture cells[1]. Similar to replicative senescence of cells, the premature form of cellular senescence can be induced by activated oncogenes, oxidase stress, telomere shortening, and DNA damage[2,3]. It is assumed that premature senescence may function as barrier mechanism against cancer progression[4-7]; in fact, many premature senescent cells have been seen in premalignant tumors[8-10].

Similar to replicative senescence, premature senescence is identified by biomarkers of senescence, *e.g.*, senescence-associated β-galactosidase (SA-β-gal). In addition to oncogenic *Ras*, premature senescence can also be induced by other oncogenes, *e.g.*, *Braf*, *AKT*, *E2F1*, *cyclin E*, *Mos*, and *Cdc6*, and by the inactivation of tumor-suppressor genes including *PTEN* and *NF1*[11]. Some oncogenes induce senescence through DNA damage responses[12], or by hyper-replication of DNA caused by sustained oncogenic signals[13,14].

Oncogene-induced senescence and replicative senescence activate tumor suppressor cascades, including p16Ink4a-Rb and p19Arf (p14ARF in human)-TP53 signaling pathways[15,16]. Though the roles of RB and TP53 signals in senescence are undisputable, other factors are also known to be involved.

Senescent cells are observed to express a vast number of secreted proteins, *e.g.,* transforming growth factor-β, insulin, Wnt, and interleukin signaling cascades protein. This phenotype was known as "senescence-associated secretory phenotype (SASP)" or "senescence-messaging secretome"[17,18]. The SASP includes many inflammatory cytokines and chemokines[17], providing a strong link between senescence and inflammation. SASP activation is largely mediated by the transcription factors nuclear factor -kB and CCAAT/enhancer-binding protein beta[19-21], and comprises a range of chemokines (chemoattractants and macrophage inflammatory proteins), proinflammatory cytokines (IL-1a, IL-1b, IL-6, and IL-8), growth factors (hepatocyte growth factor, TGFb, granulocyte-macrophage colony-stimulating factor)[22,23] and matrix-remodeling enzymes[19,20,24].

Epigenetic mechanisms are also involved in senescence. When human fibroblasts leads to cellular senescence, heterochromatic regions gather to form

senescence-associated heterochromatic foci (SAHF), in which genomic regions with histone H3K9 trimethylation condense and are surrounded by histone H3K27 trimethylation (H3K27me3). These heterochromatin foci are colocalized with heterochromatin protein HP1, macroH2A and HMGA[25]. The p16 and ARF locus is regulated by Polycomb repressive complexes (PRCs), which repress transcription in proliferating cells. The H3K27me3 mark at the locus was lost during oncogene-induced senescence, which lead to expression of *p16*^{INK4A} and *ARF* in senescence, and these molecular alterations were also observed in replicative senescence[26-29]. The histone demethylase for H3K27, Jmjd3, was reported to be critical for senescence, and knockdown of *Jmjd3* sustained repression of *p16* by H3K27me3, leading to escape from senescence[30,31].

We previously analyzed epigenetic and gene expression changes in *Ras*-induced senescence of mouse embryonic fibroblasts (MEFs) on genome-wide scale[22]. We showed that Bmp2-Smad signaling is important in *Ras*-induced senescence, and is regulated by coordinated dynamic alterations of the H3K4me3 and H3K27me3 marks. We further examined the downstream target genes of the signal genome-widely, and showed that dynamic epigenomic alteration disrupts negative feedback loop of the signal, and that continuously activated downstream targets contribute to growth arrest. These epigenetic alterations associated with Bmp2-Smad1 signal were found to occur specifically in *Ras*-activated cells, not in control cells with mock retrovirus infection[22]. In contrast, the epigenetic alteration at the *Ink4a-Arf* locus was commonly observed in *Ras*-activated cells and mock cells, *i.e.,* both in cells under *Ras*-induced senescence and cells under replicative senescence[22]. It was suggested that there might be common epigenetic mechanisms in premature senescence and replicative senescence, and also different epigenetic regulation on specific signals between the two senescence programs. Within such molecular alterations specifically observed during premature senescence, there might be some common alterations and some different alterations in premature senescence induced by different stresses, but such analysis to compare different types of premature senescence has not been conducted in detail.

Here we analyzed genome-wide transcription and epigenetic changes during *Raf*-induced senescence by microarray and ChIP-seq. We found that the majority of genes that were altered during *Ras*- and *Raf*-induced senescence were similar, and that activation of *Bmp2* and repression of *Smad6* were also involved in *Raf*-induced senescence. However, epigenetic alterations might be somewhat different between *Ras*- and *Raf*-induced senescence, *e.g.,* in gain of H3K27me3 mark at the *Smad6* locus.

MATERIALS AND METHODS

Cells and viral infection

All of the experiments were approved by from the Ethics Committee for Animal Research Studies at the University of Tokyo. The animal protocol was designed to minimize any pain or discomfort to mice. The mice were acclimatized to laboratory conditions for two weeks prior to experiments, and were euthanized by carbon dioxide inhalation for tissue collection. MEF cells were established using 13.5-embryonic-day embryos of C57/B6 mice[23]. Embryos were minced with the head and red organs removed, and digested twice with trypsin/EDTA for 15 min at 37 ℃. The cells were seeded onto 10-cm dishes and cultured in Dulbecco's modified Eagle's medium containing 100 UI/mL penicillin and 100 g/mL streptomycin sulfate, supplemented with 10% (V/V) fetal bovine serum at 37 ℃ in 50 mL/L CO_2. When cells were passed twice, the MEF cells (MEFp2) underwent retrovirus infection for 48 h. Then the cells were seeded at a density of 1×10^5 cells/6-cm dish (day 0), and total RNA was collected using TRIzol (Invitrogen, Carlsbad, CA), from MEFp2 and from virus-infected MEFs at the indicated time points.

Retroviral vectors

To induce senescence in MEF, we cloned cDNA for wild type *BRAF* (RafWT) and mutated *BRAF* (RafV600E) into a CMV promoter driven expression vector pMX-neo that contains the neomycin-resistance gene (Cell Biolabs, San Diego, CA). Using FuGENE 6 Transfection Reagent (Roche, Germany), an empty pMX-neo vector (Mock), and vectors containing RafWT and RafV600E were transfected in plat-E packaging cells (kindly gifted from T. Kitamura, the Institute of Medical Science, the University of Tokyo, Tokyo, Japan) to prepare retroviruses. The infected cells were exposed to 700 μg/mL of G418 (Invitrogen) from days 0-10 for selection. It was confirmed that MEF cells without infection completely died under these conditions by day 5. When mock-infected cells were cultured with and without G418, they did not show a difference in cellular growth, indicating that the multiplicity of infection is nearly 100%. *Smad6* cDNA with an N-terminal 6x Myc tag was cloned into pMX-puro vector in our previous study, and retroviruses were prepared using plat-E cells as above. The infected cells were exposed to 1 μg/mL of puromycin from days 0-3 for selection.

shRNA retrovirus

Using pSIREN-RetroQ Vector (Clontech, CA), a retrovirus vector to express small hairpin RNA (shRNA) against *Bmp2* was constructed as previously reported[22]. The oligonucleotide sequences targeting *Bmp2* is: GATCCG GGACACCAGGTTAGTGAAT TTCAAGAGA ATTCACTAACCTGGTGTCC CTTTTTTCTCGAGG, with the 19-mer target sense and antisense sequences underlined. Viral packaging for shRNA retrovirus vectors against *Bmp2* (shBmp2) was also performed using plat-E cells and FuGENE 6 as above. To MEFp2, RafV600E and shRNA viruses were simultaneously infected for 48 h. The infected cells were exposed to 1 μg/mL of puromycin during days 0-3 for selection.

Expression array analysis

For genome-wide gene expression analysis, GeneChip Mouse Genome 430 2.0 Array (Affymetrix) was used. Data were collected by an Affymetrix GeneChip Scanner 3000 (Affymetrix). To obtain the signal value (GeneChip score) for each probe, the GeneChip data were analyzed using Affymetrix GeneChip Operating Software v1.3 by MAS5 algorithms. The average signal in an array was made equal to 100 for global normalization. Expression array data for *Raf*-induced senescence were collected, and array data for *Ras*-induced senescence was previously submitted to GEO (#GSE18125).

Gene annotation enrichment analysis

Gene annotation enrichment was analyzed for Gene Ontology (GO) (biological process, cellular component, and molecular function) and for Functional Categories (Swiss Prot PIR database keywords, and Uniprot Sequence Feature) using the Functional Annotation tool at DAVID Bioinformatics Resources (http://david.abcc.ncifcrf.gov/).

Chromatin immunoprecipitation

MEFp2 and infected cells at day 7 were cross-linked with 1% formaldehyde for 10 min, and chromatin immunoprecipitation (ChIP) using anti-H3K4me3 (Abcam ab8580, rabbit polyclonal) and H3K27me3 (Upstate 07-142, rabbit polyclonal) was performed. Briefly, cells were crosslinked with 1% formalin for 10 min, and the crosslinked cells were sonicated for fragmentation. The fragmented samples were incubated with antibodies bound to protein A-sepharose beads at 4 ℃ overnight. The beads were then washed eight times and eluted with elution buffer. The eluates were treated with pronase at 42 ℃ for 2 h and then underwent incubation at 65 ℃ overnight to reverse the crosslinks. The immunoprecipitated DNA was purified by the phenol/chloroform procedure and precipitated with LiCl and 70% ethanol.

ChIP-sequencing

Samples for ChIP-sequencing were prepared according to the manufacturer's instructions by Illumina, and sequencing was performed using Solexa Genome Analyzer Ⅱ. By using the Illumina pipeline software v1.4, 36-bp single-end sequence reads were mapped to the reference mouse genome NCBI Build #36 (UCSC mm8). The numbers of uniquely mapped reads were 10845082 (H3K4me3), 11519151 (H3K27me3), and 5688804 (Input) for MEFp2, and were 26339875 (H3K4me3), 27239707 (H3K27me3), and 6126206 (Input) for RafV600E cells. ChIP-seq data for *Ras*-induced senescence was previously submitted to GEO (#GSE18125).

To determine the distribution of immunoprecipitated DNA fragments in a certain region, we set a window in genomic DNA, within which we counted a number of uniquely mapped Solexa reads, as previously performed[22]. A window size of 300 bp was used in ChIP-seq of H3K4me3, and that of 500 bp for H3K27me3, because H3K4me3 was distributed in narrow DNA regions and 300 bp was wide enough for a window, but H3K27me3 is rather broad modification than H3K4me3, so a wider window, 500 bp, was necessary to detect read count. To express the modification status for the center position of the window, the number of mapped reads per 1000000 reads within a window was counted and calculated. Within ± 2 kb from the TSS of each gene, the maximum number of mapped reads per 1000000 reads in a window was adopted as the modification status of each gene. When the number was > 3.5 and < 3 for H3K4me3, the gene was regarded as H3K4me3(+) and (-), respectively. When the number was > 1.5 and < 1 for H3K27me3, the gene was regarded as H3K27me3(+) and (-), respectively.

SA-β-gal analysis

MEFp2 and infected cells on days 3, 5, 7 and 10 underwent SA-β-gal staining[32]. Cells were washed with PBS twice, and incubated in fixation buffer [2% (w/v) formaldehyde, 0.2% (w/v) glutaraldehyde in PBS] for 5 min. The cells were washed with PBS twice again, then incubated in the SA-β-gal staining solution (40 mmol/L citric acid/sodium phosphate, pH 6.0, 150 mmol/L NaCl, 2.0 mmol/L MgCl2, 5 mM K4[Fe(CN)6], 5 mmol/L K3[Fe(CN)6], 1 mg/mL X-gal) overnight.

Growth curve

The infected cells were counted on days 3, 5, 7, and 10 using the Countess cell counter (Invitrogen). A growth curve was drawn by calculating mean number of three dishes.

Quantitative real-time RT-PCR and ChIP-PCR

For RT-PCR, the total RNA was treated with DNase Ⅰ (Invitrogen), and cDNA was synthesized from 1 μg of total RNA using a Superscript Ⅲ kit (Invitrogen). Real-time RT-PCR was performed using SYBR Green and iCycler Thermal Cycler (Bio-Rad Laboratories). The number of molecules of *BRAF*, *Bmp2* and *Smad6* in a sample was measured by comparing with the standard samples containing 10^1 to 10^6 copies of the genes. The quantity of mRNA of each gene was normalized to that of *Ppib*, and the relative expression levels compared to those in RafV600E were shown. The experiment was performed three times and the mean and standard error were calculated and shown. The following PCR primers were used. *BRAF*: CACCATCTCC ATATCATTGA GACCA and CGAGATTTCA CTGTAGCTAG ACCAA. *Bmp2*: TATCATGCCT TTTACTGCCA and ATTCACAGAG TTCACCAGAG TC. *Smad6*: ATCCCCAAGC CAGACAGTCC and TCCTTGAGCC TCTTGAGCAG C. *Ppib*: ATGTGGTACG GAAGGTGGAG A and AGCTGCTTAG AGGGATGAGG.

For ChIP-PCR, real-time PCR using SYBR Green and iCycler Thermal Cycler (Bio-Rad Laboratories) was performed to amplify ChIP samples, and they were

quantified by comparing with the standard samples, *i.e.,* 20, 2, 0.2, and 0.02 ng/μL of sonicated genomic DNA of MEF. The following PCR primers were used. *Actb*: TGAGGTACTA GCCACGAGAG AG and ACACCCGCCA CCAGGTAAGC A. *Gcgr*: TGCTGTCATG TCTGGTGAGT G and GGAGCTGTCA GCACTTGTGT A. *Bmp2*: CTTGGCTGGA GACTTCTTGA ACT and TGGAGGCGGC AAGACTGGAT. *Smad6*: CTGGGGTTTG GAATGCCTAA and CTAAAAGCTA TGTACCGACT GAGG.

Statistical analysis

Unsupervised two-way hierarchical clustering was performed using the Cluster 3.0 software (Stanford University, http://bonsai.ims.u-tokyo.ac.jp/~mdehoon/software/cluster/software.htm#ctv). A heat map was drawn by Java TreeView software (Alok, http://jtreeview.sourceforge.net/). Fisher's exact test, Student's *t*-test, Kolmogorov-Smirnov test, phi coefficient analysis, and log linear analysis were performed using R software (http://www.R-project.org/).

RESULTS

Gene expression analysis

MEF cells after two passages (MEFp2) were infected with retrovirus of wild type *Raf* (RafWT) or oncogenic *Raf* (RafV600E), or mock retrovirus, and cultured through day 10 (Figure 1). While mock cells showed cellular growth similar to that of MEF cells without infection and RafWT cells showed slightly but significantly faster growth than those, RafV600E cells hardly showed cellular growth (Figure 1B).

SA-β-gal staining was performed on RafV600E cells on days 3, 5, 7, and 10, and the number of SA-β-gal(+) cells was counted and compared with those for MEF cells without retrovirus infection, mock cells and RafWT cells. RafV600E cells showed a marked increase in number of SA-β-gal(+) cells after day 5, but the number of mock cells and RafWT cells did not increase until day 10 (Figure 1C and D). When cells were infected with retrovirus of oncogenic *Ras* (RasG12V) and wild type *Ras* (RasWT) as previous study[22], RasG12V cells showed a marked increase of SA-β-gal(+) cells after day 7, while RasWT cells did not until day 10 (Figure 1D).

Gene expression analysis was performed on genome-wide scale using expression array, and gene expression changes in *Raf*-induced senescence were compared with those in *Ras*-induced senescence (Figure 2). A two-way hierarchical clustering analysis was performed for genes showing > 5-fold increase or < 0.2-fold decrease in any samples of *Ras*-induced senescence and *Raf*-induced senescence compared with MEFp2. The major cluster of upregulated genes contained three subgroups: Genes upregulated by *Ras* and *Raf* commonly, by *Ras* specifically, and by *Raf* specifically. Though it is less clear, the cluster of downregulated genes also showed three similar subgroups: Genes downregulated by *Ras* and *Raf* commonly, by *Ras* specifically, and by *Raf* specifically.

We previously reported that epigenetic activation of *Bmp2* and repression of *Smad6* is important in *Ras*-induced senescence. *Bmp2* was included in the subgroup of genes upregulated by *Ras* and *Raf* commonly, and *Smad6* was included among those that were downregulated by *Ras* and *Raf* commonly.

Comparison of genes upregulated/downregulated in Ras-/Raf-induced senescence

We performed GO enrichment analysis for 841 genes showing > 5-fold increase in RasV12 cells and RafV600E cells commonly (Figure 3A). Genes associated with signal/secreted proteins ($P = 3.8 \times 10^{-30}$), extracellular regions ($P = 5.3 \times 10^{-19}$), and cell differentiation/development ($P = 6.1 \times 10^{-9}$) were upregulated, *e.g., Bmp2* and *Igfbp3*, supporting the alteration of secreted factor expression during senescence, and these factors might play a common role in *Ras*- and *Raf*-induced senescence. The 573 genes showing < 0.2-fold decrease commonly RasV12 cells and RafV600E cells, showed genes related to cell cycle ($P = 1.3 \times 10^{-33}$) such as *Cdc6*, in good agreement with growth arrest (Figure 3B). Genes related to secreted protein ($P = 2.0 \times 10^{-12}$) and extracellular region ($P = 5.4 \times 10^{-13}$), such as *Cxcl5* and *Wnt4*, were also enriched, suggesting that the dynamic activation and repression of some secreted factors occur commonly during *Ras*- and *Raf*-induced senescence. The GO-term "protein binding" also showed significant enrichment, and *Smad6* was included in this term.

Genes altered in Ras-/Raf-induced senescence and also in mock cells

Among these genes altered commonly during *Ras*- and *Raf*-induced senescence, some genes showed similar alteration patterns in mock cells (Figure 4). There were 348 genes showing > 5-fold upregulation commonly in mock cells, RasG12V cells and RafV600E cells, compared with MEF. Genes associated with signal/secreted proteins proteins ($P = 6.7 \times 10^{-12}$) or extracellular regions ($P = 3.3 \times 10^{-9}$), *e.g., Igfbp3* and *Cd5l*, were significantly enriched in these genes, suggesting the involvement of common secreted factors in both oncogene-induced senescence and replicative senescence (Figure 4A). Similarly, there were 80 genes, *e.g., Cdc6* and *Wnt4*, showing < 0.2-fold downregulation commonly in mock cells, RasG12V cells and RafV600E cells, compared with MEF (Figure 4B).

Genes altered in Ras-/Raf-induced senescence but not in mock cells

In some genes, in contrast, the expression alterations commonly observed in *Ras-/Raf*-induced senescence did not occur in mock cells (Figure 5). There were 259 genes showing > 5-fold upregulation commonly in RasG12V cells and RafV600E cells, but not in mock cells. Genes associated with signal/secreted proteins ($P = 1.8 \times 10^{-10}$) or extracellular regions ($P = 7.0 \times 10^{-5}$), *e.g., Bmp2*, were also significantly enriched in these

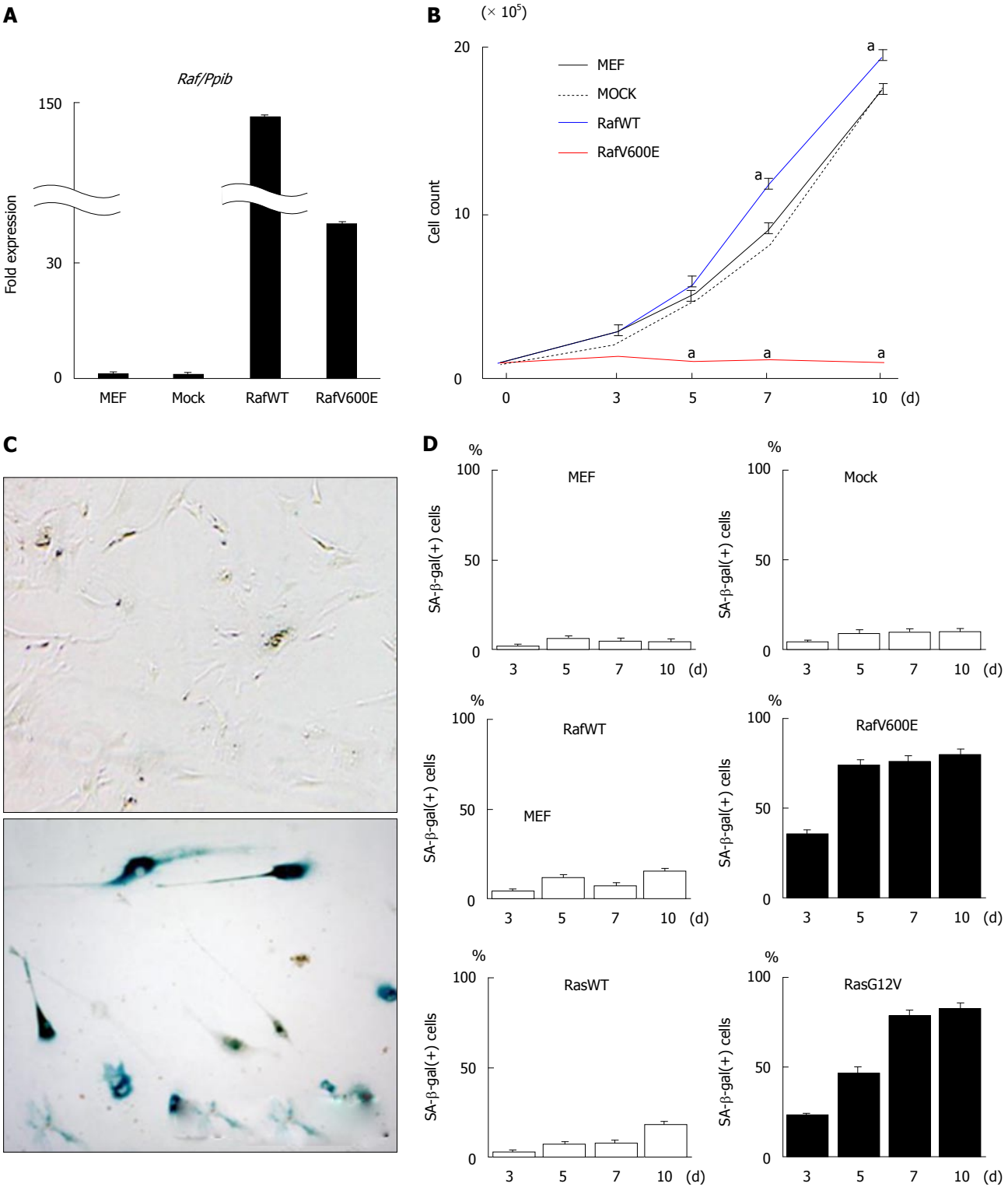

Figure 1 Induction of cellular senescence in mouse embryonic fibroblast by oncogenic *Raf*. A: Induction of *Raf* by retroviral infection. Retrovirus was infected to MEFs on day -2 to induce the expression of wild type *Raf* (RafWT) or oncogenic *Raf* (RafV00E). RNA was collected on day 7, and the expression level of BRAF was analyzed by real-time RT-PCR to confirm expression induction; B: Growth curve. Retrovirus was infected into MEFs on day -2. After two days (day 0), the cell number was counted to draw the growth curve. Cells that were infected with mock retrovirus Mock cells (black dotted line) showed cellular growth similar to that of MEF cells without infection (black line), and RafWT cells (blue line) showed slightly but significantly faster growth than did MEF cells without infection. RafV600E cells hardly showed cellular growth (red line). $^{a}P < 0.05$ (t); C: SA-β-gal staining. Compared with MEF cells on day 7 (above), RafV600E cells on day 7 (bottom) showed positive staining of SA-β-gal; D: Count of SA-β-gal(+) cells. The number of SA-β-gal(+) cells was counted on days 3, 5, 7, and 10. MEF cells without virus infection rarely showed SA-β-gal(+) cells. While mock cells and RafWT cells did not show a marked increase in the number of SA-β-gal(+) cells, RafV600E cells showed a marked increase in the number of SA-β-gal(+) cells after day 5 (73.3% ± 2.9% on day 5). When cells were infected with retrovirus of oncogenic *Ras* (RasG12V) and wild type *Ras* (RasWT) as previous study[22], RasG12V cells showed marked increase of SA-β-gal(+) cells after day 7 (showed 78.3% ± 4.5% on day 7), while RasWT cells did not until day 10. The mean and standard error in three repeated experiments were shown. MEF: Mouse embryonic fibroblast.

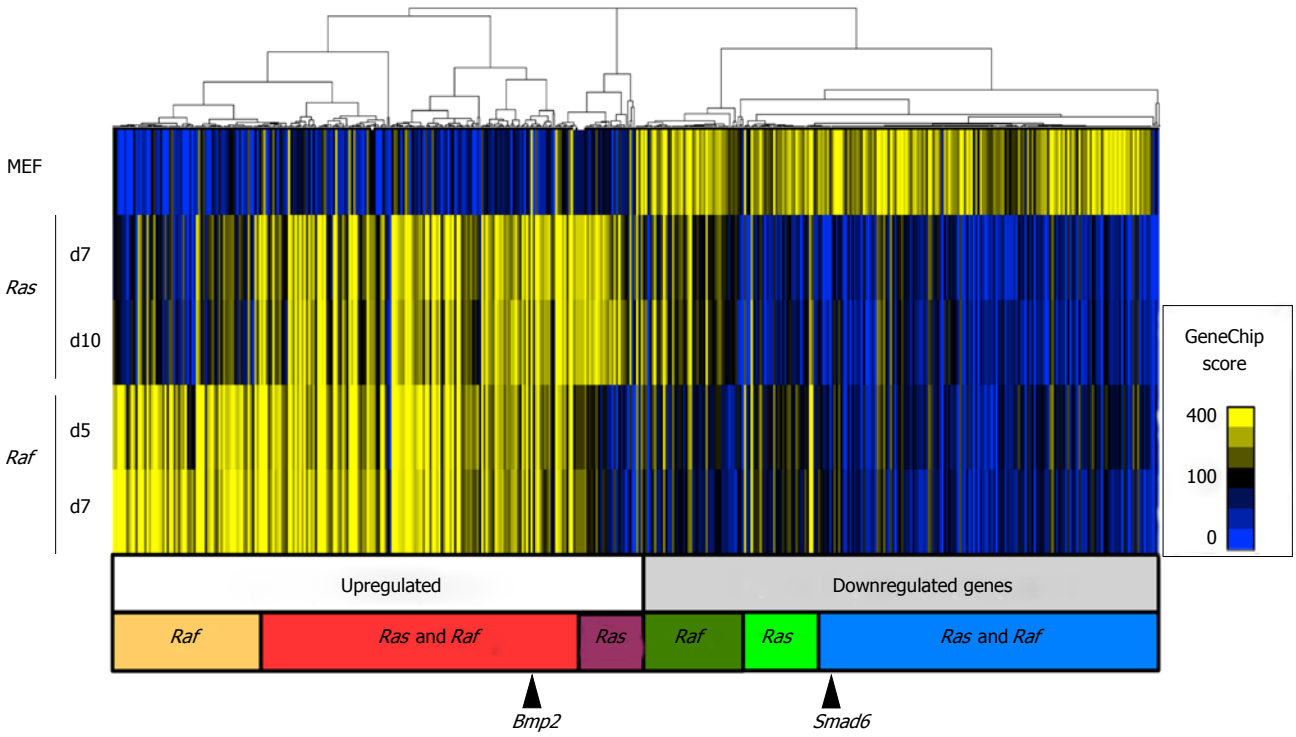

Figure 2 Hierarchical clustering analysis of genes altering expression levels during senescence. Gene expression levels were analyzed for 15653 genes using microarray for MEF cells, and RafV600E cells on days 5 and 7. For senescence induced by oncogenic *Ras* (RasG12V), RasG12V cells on days 7 and 10 were analyzed in our previous study, and compared with *Raf*. A total of 729 probes showing an expression level higher than 100 in GeneChip score in any of the five samples, and showing either > 5-fold upregulation or > 0.2-fold downregulation in any RafV600E or RasG12V samples compared with MEF, were extracted for clustering analysis. The major cluster for upregulated genes consisted of three subclusters: Genes upregulated specifically in *Raf*-induced senescence, those commonly upregulated in *Ras*- and *Raf*-induced senescence, and those upregulated specifically in *Ras*-induced senescence. The other major cluster for downregulated genes also contained three subgroups of genes, albeit not very clear: Genes downregulated specifically in *Raf*-induced senescence or *Ras*-induced senescence, and those commonly downregulated in *Ras*- and *Raf*-induced senescence. *Bmp2* was included in commonly upregulated genes and *Smad6* was included in commonly downregulated genes (black arrows). MEF: Mouse embryonic fibroblast.

genes, suggesting involvement of some secreted factors specifically in oncogene-induced senescence, but not in replicative senescence (Figure 5A). Similarly there were 242 genes, *e.g., Smad6*, showing < 0.2-fold downregulation commonly in RasG12V cells and RafV600E cells, but not in mock cells. Genes associated with signal/secreted protein ($P = 2.3 \times 10^{-17}$) or extracellular region ($P = 1.3 \times 10^{-17}$) were also significantly enriched in these genes, *e.g., Cxcl5* (Figure 5B). Interestingly, these GO terms were not enriched in genes commonly downregulated in mock, RasG12V, and RafV600E cells (Figure 4B), suggesting that repression of secreted factors occur more dynamically during *Ras*- and *Raf*-induced senescence, than in replicative senescence.

Genes altered specifically either in Ras- or Raf-induced senescence

Some genes altered specifically in RasG12V cells, but not in mock cells and RafV600E cells, including 36 upregulated and 167 downregulated genes. The 167 downregulated genes showed a significant enrichment of genes associated with signal/secreted proteins, *e.g., Wnt2* (Figure 6A and B). Similarly, some genes altered specifically in RafV600E, but not in mock cells and RasG12V cells, including 63 upregulated and 170 downregulated genes. These genes showed significant enrichment of GO-terms such as "secreted" and "membrane", *e.g., Cd40* in upregulated genes and *Mcam* in downregulated genes (Figure 6C and D). These results suggested that some environment of secreted proteins might be specifically induced by *Ras*- or *Raf*-induced senescence.

Increase of Bmp2 and decrease of Smad6

We previously reported that the activation of Bmp2-Smad signaling by the harmonized epigenetic activation of *Bmp2* and repression of *Smad6* contributes to *Ras*-induced senescence[22]. In the present study, *Bmp2* and *Smad6* were found to be altered commonly in *Ras*- and *Raf*-induced senescence, but not in mock cells (Figure 5). In our recent targeted exon sequencing analysis in colorectal tumors, mutation of genes in BMP signaling, *e.g., BMPR2*, *BMP2*, and *SMAD4*, were significantlydetected in *BRAF*-mutation(+) colorectal cancer[33]. It was thus suggested that activation of Bmp2-Smad signalling might be also critical in Raf-induced senescence and disruption of the signaling may play a role in tumorigenesis of *BRAF*-mutation(+) colorectal cancer. To examine whether an increase of *Bmp2* and decrease of *Smad6* contributed to *Raf*-induced

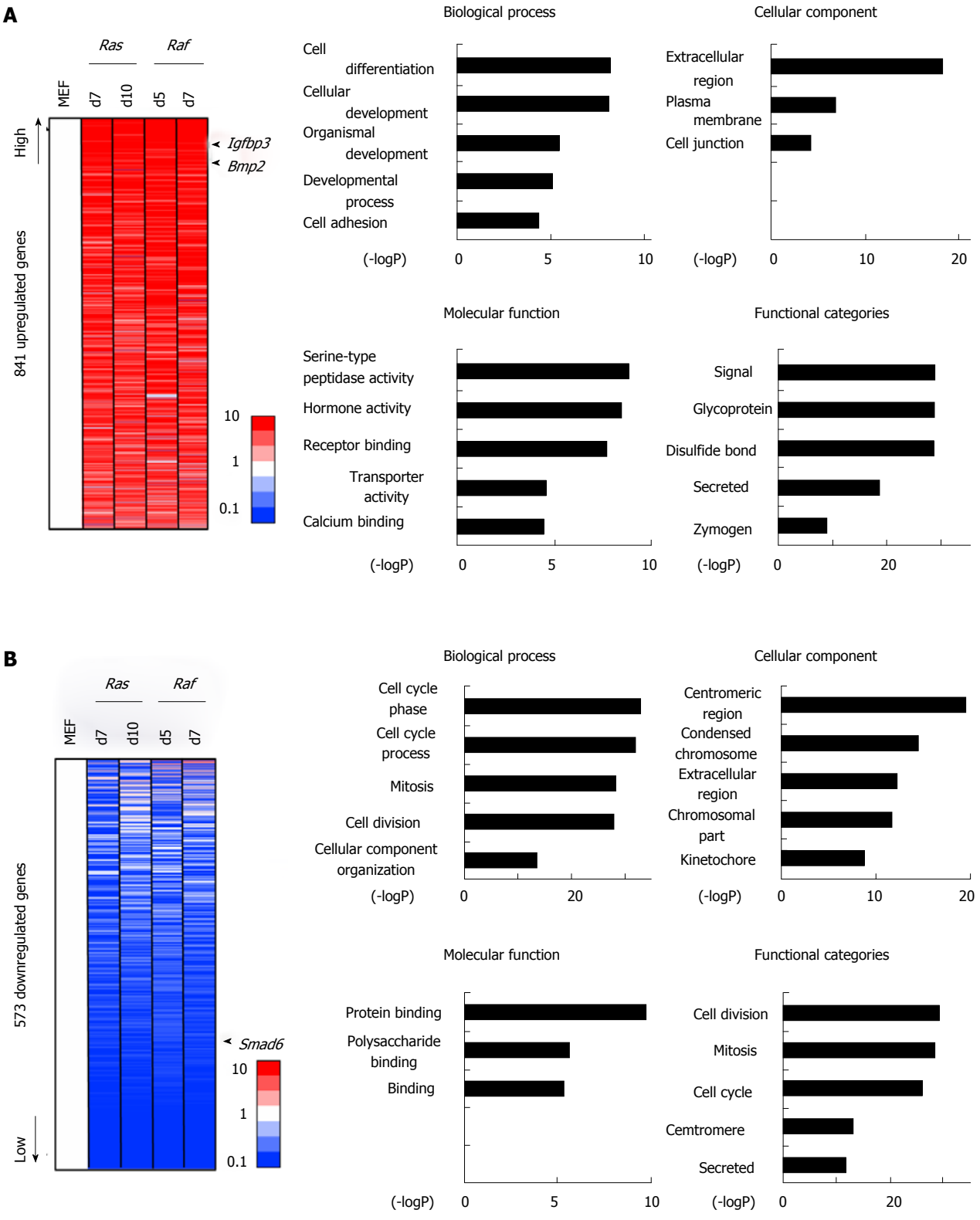

Figure 3 Gene annotation enrichment analysis for commonly altered genes. A: Commonly upregulated genes. A total of 841 genes showed > 5-fold upregulation commonly in either of RasG12V cells on days 7 (*Ras d7*) and 10 (*Ras d10*) and in either of RafV600E cells on days 5 (*Raf d5*) and 7 (*Raf d7*), compared with MEF. More upregulated genes were sorted upward. Gene annotation enrichment was analyzed for biological process, cellular component, molecular function, and functional categories. Genes associated with signal/secreted proteins ($P = 3.8 \times 10^{-30}$), extracellular regions ($P = 5.3 \times 10^{-19}$), and cell differentiation/development ($P = 6.1 \times 10^{-9}$), *e.g.*, *Bmp2* and *Igfbp3*, were upregulated; B: Commonly downregulated genes. A total of 573 genes showed < 0.2-fold downregulation commonly in either of the two RasG12V cells and in either of the two RafV600E cells, compared with MEF. More downregulated genes were sorted downward. Gene annotation enrichment analysis showed that genes related to cell cycle ($P = 1.3 \times 10^{-33}$) such as *Cdc6* were significantly enriched, in good agreement with growth arrest. Genes associated with secreted protein ($P = 2.0 \times 10^{-12}$) and extracellular region ($P = 5.4 \times 10^{-13}$) such as *Cxcl5* and *Wnt4* were also enriched, suggesting that the dynamic activation and repression of secreted factors occurred commonly during *Ras*- and *Raf*-induced senescence. The GO-term "protein binding" also showed significant enrichment, and *Smad6* was included in this term. MEF: Mouse embryonic fibroblast.

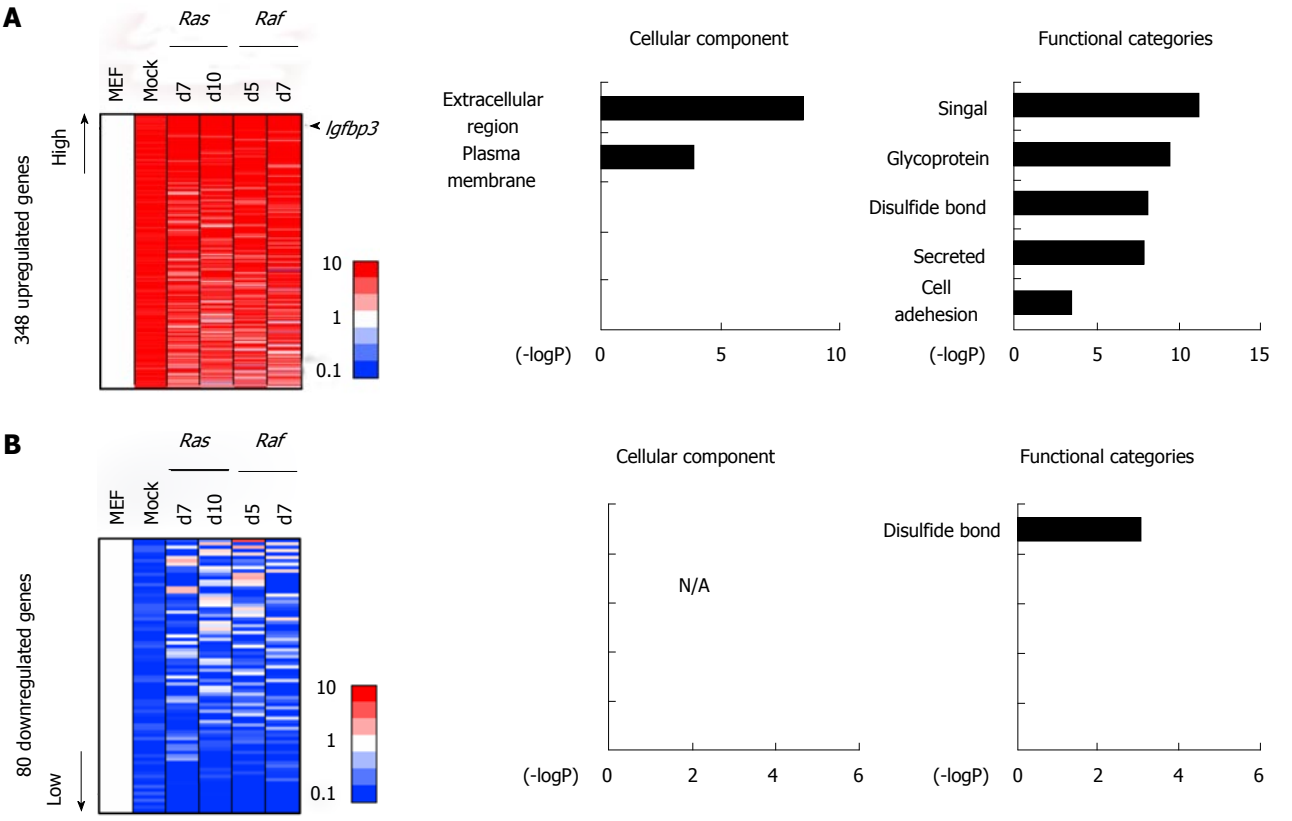

Figure 4 Genes altered commonly in *Ras*-/*Raf*-induced senescence and in mock cells. A: Commonly upregulated genes. There were 348 genes showing > 5-fold upregulation commonly in mock cells, in either of the two RasG12V cells and in either of the two RafV600E cells, compared with MEF. Genes associated with signal/secreted proteins proteins ($P = 6.7 \times 10^{-12}$) or extracellular regions ($P = 3.3 \times 10^{-9}$), *e.g.*, *Igfbp3* and *Cd5l*, were significantly enriched in these genes. B: Commonly downregulated genes. There were 80 genes, *e.g.*, *Cdc6* and *Wnt4*, showing < 0.2-fold downregulation commonly in mock cells, in either of two RasG12V cells and in either of two RafV600E cells, compared with MEF. Genes related to disulfide bond were significantly enriched. MEF: Mouse embryonic fibroblast.

senescence, a retrovirus to express shRNA against *Bmp2* (shBmp2) or retrovirus to express *Smad6* was infected together with RafV600E infection (Figure 7A). When *Bmp2* was knocked down, RafV600E cells showed escape from senescence with number of SA-β-gal(+) cells decreased (Figure 7B and C). *Smad6* expression also caused escape from senescence with number of SA-β-gal(+) cells decreased (Figure 7B and D). These indicated that increase of *Bmp2* and decrease of *Smad6* also play an important role in *Raf*-induced senescence, as well as *Ras*-induced senescence.

In *Ras*-induced senescence, while the *Bmp2* promoter region gained H3K4me3 mark and lost H3K27me3 mark, the *Smad6* promoter region gained H3K27me3 mark and lost H3K4me3 mark in opposite manner. To examine epigenomic alteration of these histone modifications in *Raf*-induced senescence, ChIP analysis for H3K4me3 and H3K27me3 was performed for RafV600E cells (Figure 8). In the *Bmp2* promoter, gain of H3K4me3 and loss of H3K27me3 were detected in *Raf*-induced senescence as well as in *Ras*-induced senescence. In the *Smad6* promoter, however, loss of H3K4me3 was detected in *Raf*-induced senescence while de novo H3K27me3 induction was not detected. These results indicated that decrease of *Smad6* involved loss of H3K4me3, but did not involve PRC2 recruitment to the promoter region, and suggested that epigenetic alteration might be somewhat different between *Ras*- and *Raf*-induced senescence.

Integrated analysis of epigenetic alteration and expression

To compare histone modification alterations between *Ras*- and *Raf*-induced senescence on genome-wide scale, we performed integrated analyses of epigenetic and expression alterations (Figure 9). Among the analyzed 20232 genes with epigenetic alteration, 15653 genes were also analyzed for expression on microarray, and for integrated analyses. For epigenetic status of H3K27me3, 483 genes showed > 1.5 reads per 1000000 reads in MEFp2, but decreased to < 1.0 reads per 1000000 reads in both or either of *Ras*- and *Raf*-induced senescence. Among these 483 genes losing H3K27me3 in senescence, 27 genes in *Ras*-induced senescence and 18 genes in *Raf*-induced senescence showed a simultaneous loss of H3K27me3 and gain of H3K4me3 (with increase from < 3.0 reads in MEFp2 to > 3.5 reads in senescence), and 9 genes, including *Bmp2*, showed simultaneous H3K27me3 loss and H3K4me3 gain in both senescence mechanisms. These genes showed significant enrichment in upregulated genes among the 483 genes ($P = 1 \times 10^{-5}$ in *Ras*-

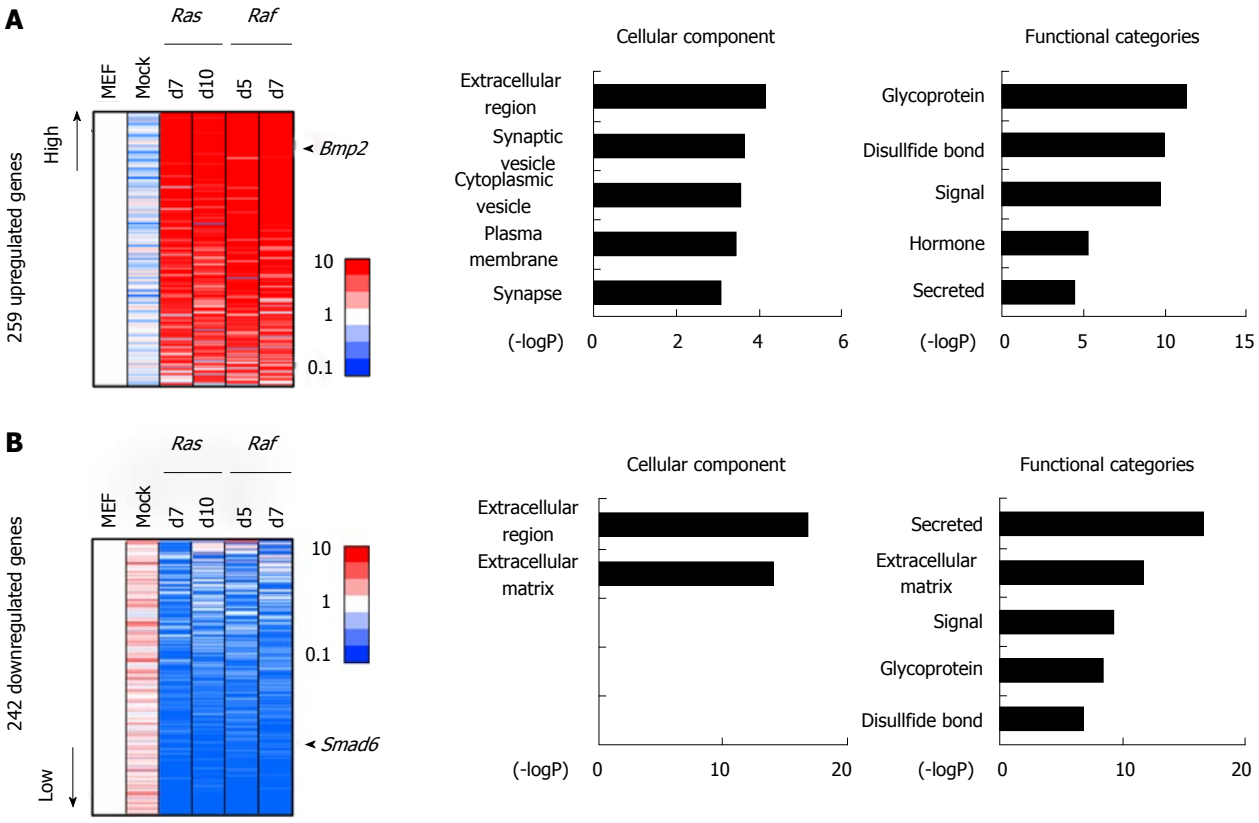

Figure 5 Genes altered commonly in *Ras*-/*Raf*-induced senescence but not in mock cells. A: Genes upregulated commonly, but not in mock cells. There were 259 genes showing > 5-fold upregulation commonly in either of the two RasG12V cells and in either of the two RafV600E cells, but not in mock cells. Genes associated with signal/secreted proteins ($P = 1.8 \times 10^{-10}$) or extracellular regions ($P = 7.0 \times 10^{-5}$), *e.g.*, *Bmp2*, were significantly enriched in these genes; B: Genes downregulated commonly, but not in mock cells. There were 242 genes, *e.g.*, *Smad6*, showing < 0.2-fold downregulation commonly in either of the two RasG12V cells and in either of the two RafV600E cells, but not in mock cells. Genes associated with signal/secreted protein ($P = 2.3 \times 10^{-17}$) or extracellular region ($P = 1.3 \times 10^{-17}$) were significantly enriched, *e.g.*, *Cxcl5*.

induced senescence, $P = 2 \times 10^{-9}$ in *Raf*-induced senescence, and $P = 2 \times 10^{-8}$ in both senescence, Kolmogorov-Smirnov test, Figure 9).

In contrast, 240 genes showed < 1.0 reads per 1000000 reads in MEFp2, but increased to > 1.5 reads per 1000000 reads in both or either *Ras*- and *Raf*-induced senescence (Figure 10A). Among these 240 genes acquiring *de novo* H3K27me3 in senescence, 10 genes in Ras-induced senescence (like *Smad6*) and 7 genes in Raf-induced senescence showed simultaneous gain of H3K27me3 and loss of H3K4me3, and these genes showed significant enrichment in downregulated genes among the 240 genes ($P = 4 \times 10^{-6}$ in *Ras*-induced senescence, $P = 0.02$ in *Raf*-induced senescence, Kolmogorov-Smirnov test, Figure 10A). However, the 10 genes and 7 genes did not overlap at all, including *Smad6*.

Regarding the overlap of H3K27me3 alterations, 171 genes with H3K27me3 loss in *Ras*-induced senescence and 417 genes with H3K27me3 loss in *Raf*-induced senescence showed significant overlap (105 genes, $P < 1 \times 10^{-15}$, phi coefficient = 0.386). However, 185 genes with H3K27me3 gain in *Ras*-induced senescence and 67 genes with H3K27me3 gain in *Raf*-induced senescence showed limited overlap (12 genes only, phi coefficient = 0.103), and the latter overlap in H3K27me3 gain was markedly rare compared with the former overlap in H3K27me3 loss ($P < 1 \times 10^{-15}$, log linear analysis).

Regarding the overlap of H3K4me3 alterations, genes with H3K4me3 gain in *Ras*- and *Raf* induced senescence showed a significant overlap (50 genes, $P < 1 \times 10^{-15}$, phi coefficient = 0.413), and also genes with H3K4me3 loss in *Ras*- and *Raf*-induced senescence showed a significant overlap (380 genes, $P < 1 \times 10^{-15}$, phi coefficient = 0.559) (Figure 10B). The overlap in H3K27me3 gain was again markedly rare, when compared with the overlap in H3K4me3 gain ($P = 2 \times 10^{-9}$, log linear analysis) or with that in H3K4me3 loss ($P < 1 \times 10^{-15}$, log linear analysis).

DISCUSSION

In this study, we examined epigenomic and gene expression alterations during *Raf*-induced senescence, comparing them with alterations during *Ras*-induced senescence. The expression of many genes was commonly altered between *Ras*- and *Raf*- induced senescence, including genes related to secreted proteins and cell cycle. *Bmp2* upregulation and *Smad6* downregulation were observed and played a role in *Raf*-induced

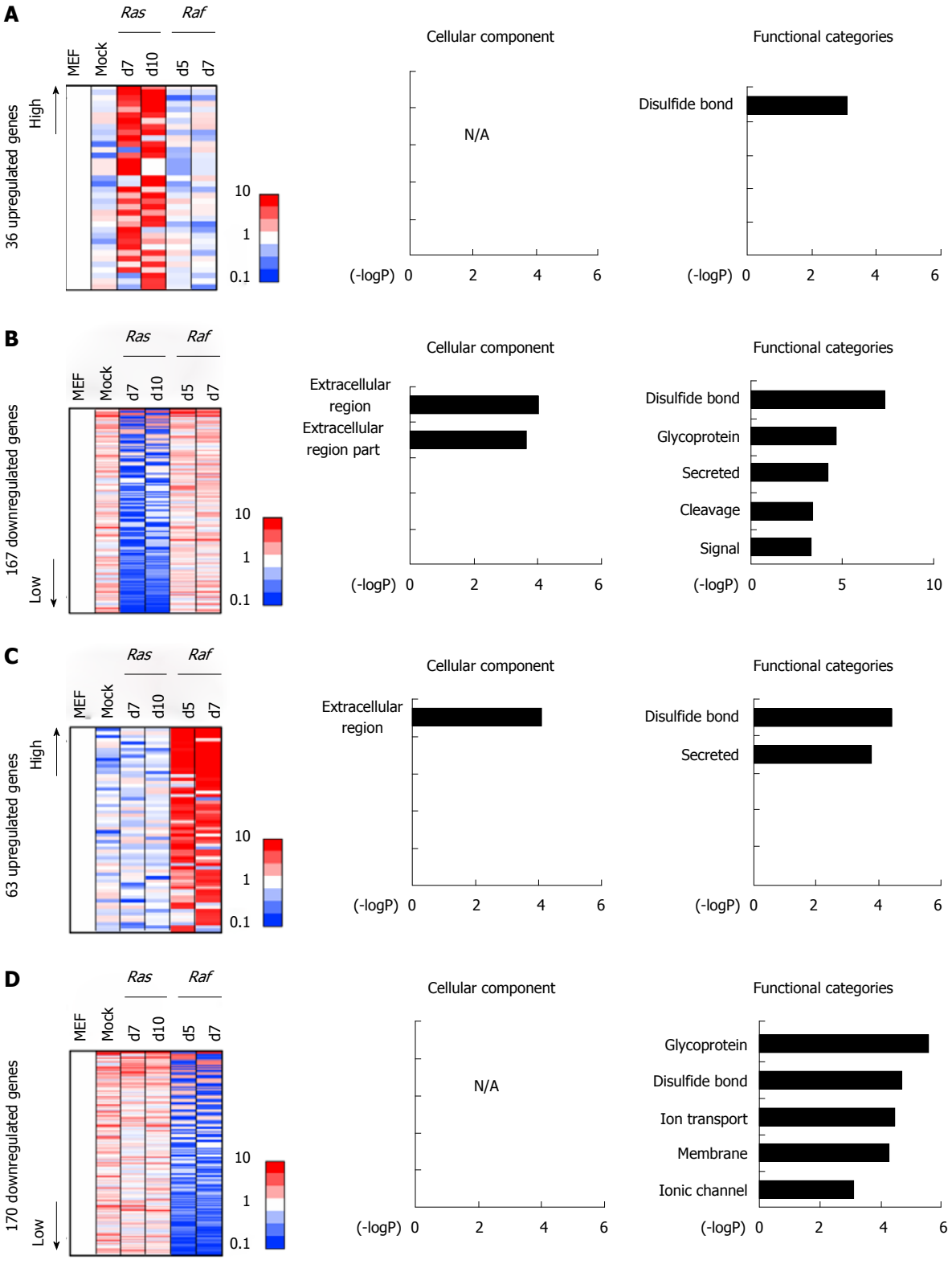

Figure 6 Gene annotation enrichment analysis for specifically altered genes. A: Genes specifically upregulated in *Ras*-induced senescence. A total of 36 genes showed > 5-fold expression in either of the two RasG12V cells, but showed < 1.5-fold expression in both RafV600E cells and in mock cells, compared with MEF cells. Gene annotation enrichment analysis did not reveal any significant enrichment of GO-terms other than "disulfide bond"; B: Genes specifically downregulated in *Ras*-induced senescence. A total of 167 genes showed < 0.2-fold expression in either of the two RasG12V cells, but showed > 0.65-fold expression in both RafV600E cells and in mock cells, compared with MEF cells. Gene annotation enrichment was analyzed, showing a significant enrichment of genes associated with signal/secreted factors, *e.g.*, *Wnt*; C: Genes specifically upregulated in *Raf*-induced senescence. A total of 63 genes showed > 5-fold expression in either of the two RafV600E cells, but showed < 1.5-fold expression in both RasG12V cells and in mock cells, compared with MEF cells. Gene annotation enrichment analysis showed significant enrichment of genes associated with secreted proteins, *e.g.*, *Cd40*; D: Genes specifically downregulated in *Raf*-induced senescence. A total of 170 genes showed < 0.2-fold expression in either of the two RafV600E cells, but showed > 0.65-fold expression in both RasG12V cells and in mock cells, compared with MEF cells. Gene annotation enrichment analysis showed a significant enrichment of genes related to membrane, *e.g.*, *Mcam*. MEF: Mouse embryonic fibroblast.

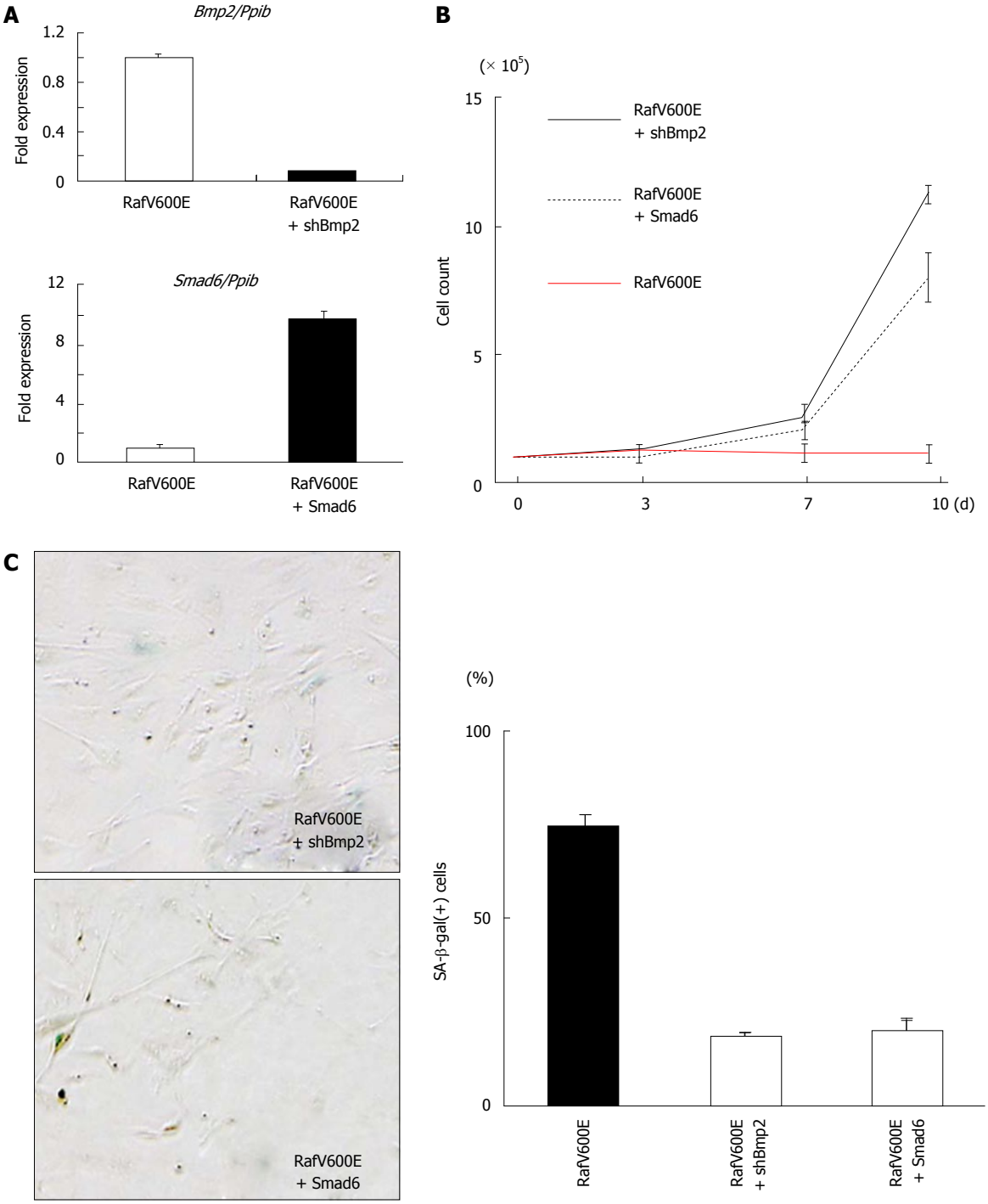

Figure 7 Knockdown of *Bmp2* and overexpression of *Smad6* inhibited growth arrest by *Raf*. A: Real-time-PCR for *Bmp2* and *Smad6*, normalized to *Ppib*. Fold expression levels compared to RafV600E cells are shown. Knockdown of *Bmp2* expression by shRNA and induction of *Smad6* expression by retrovirus infection were confirmed. Mean and standard error in triplicated samples are shown; B: Growth curve of RafV600E + shBmp2 and RafV600E + *Smad6* cells. While RafV600E cells showed growth arrest, *Bmp2*-knocked-down RafV600E cells (RafV600E + shBmp2, black line) and *Smad6*-overexpressed RafV600E cells (RafV600E + Smad6, black dotted line) showed continual growth and escape from *Raf*-induced senescence; C: Count of SA-β-gal(+) cells. Compared with RafV600E cells, *Bmp2*-knocked-down RafV600E cells (RafV600E + shBmp2) and *Smad6*-overexpressed RafV600E cells (RafV600E + Smad6) rarely showed SA-β-gal(+) cells. Mean and standard error in three repeated experiments are shown. SA-β-gal: Senescence-associated β-galactosidase.

senescence as well as *Ras*-induced senescence. But there were clusters of genes showing expression altered specifically in either *Ras*- or *Raf*-induced senescence, and epigenetic alteration might also be somewhat different, *e.g.*, in gain of H3K27me3.

Ras- and *Raf*-induced senescence share several features. SAHF formation was observed in the cellular senescence of human fibroblasts, by both *Ras*- and *Raf*-activation[34,35]. Growth arrest induced by *Ras* and *Raf* is accompanied by accumulation of TP53 and p16, and was reported to be phenotypically indistinguishable from replicative senescence[2,36-38]. Regarding SASP,

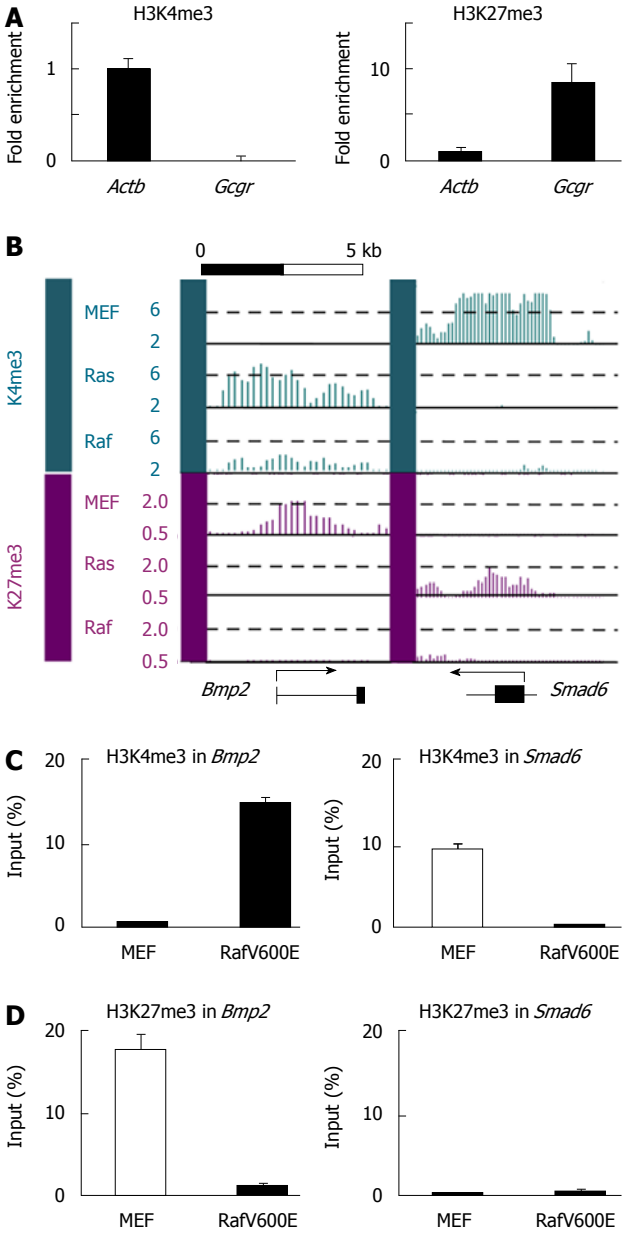

Figure 8 Epigenetic alteration of the *Bmp2* and *Smad6* locus in *Raf*-induced senescence. A: Real-time ChIP-PCR for H3K4me3 and H3K27me3 in RafV600E cells on day 7. Relative enrichment compared with *Actb* was shown, and it was confirmed that ChIP was performed properly. *Actb* was positive control region for H3K4me3 and *Gcgr* was positive control for H3K27me3; B: H3K4me3 and HK27me3 mapped by ChIP-sequencing. Y-axis, the number of mapped reads per 1000000 reads, within a window (300bp for H3K4me3 and 500bp for H3K27me3). The *Bmp2* locus showed H3K27me3 mark, but no H3K4me3 mark, in MEF cells. Loss of H3K27me3 and gain of H3K4me3 were detected commonly in *Ras*- and *Raf*-induced senescence. The *Smad6* locus showed H3K4me3 mark, but no H3K27me3 mark, in MEF cells. Loss of H3K4me3 was detected commonly in *Ras*- and *Raf*-induced senescence, but gain of H3K27me3 was detected specifically in *Ras*-induced senescence; C: Validation of the epigenetic status of the *Bmp2* locus by ChIP-PCR. Loss of H3K27me3 and gain of H3K4me3 in RafV600E cells were confirmed. We repeated ChIP assay twice, and obtained the similar results by ChIP-PCR using those ChIP products; D: Validation of the epigenetic status of the *Smad6* locus by ChIP-PCR. Loss of H3K4me3 and no gain of H3K27me3 in RafV600E cells were confirmed. We repeated ChIP assay twice, and obtained the similar results by ChIP-PCR using those ChIP products. MEF: Mouse embryonic fibroblast.

while cytokines *e.g.,* IL-6 and IL-8 are upregulated and secreted by senescent cells in a paracrine fashion in *Ras*-induced senescence[24], IL-6 and IL-8 are also secreted and play a role in *Raf*-induced senescence[19]. In *Ras*- and *Raf*-induced senescence in primary melanocytes, pigment epithelium-derived factor and Microphthalmia-associated transcription factor were commonly downregulated[39].

In this study, genes related to secreted factors, including *Igfbp3* and *Cd5l*, were commonly upregulated in *Ras*- and *Raf*-induced senescence, and also in mock cells (Figure 4A). In ageing cells, *Igfbp3* and *Cd5l* were reported to be upregulated and contribute to cellular senescence. Genes downregulated commonly in *Ras*- and *Raf*-induced senescence and in mock cells (Figure 4B) also included interesting genes. Cdc6 suppresses $p16^{INK4a}$ function, and the knockdown of Cdc6 induces senescence in cancer cells. Downregulation of *Wnt4* expression and activation of repressor pathways to suppress β-catenin dependent signaling were reported to play a role in the initiation of age-related senescence of thymic epithelial cells[40]. Alteration of these genes may play a role in both *Ras*- and *Raf*-induced senescence.

Some genes showed expression alteration commonly in *Ras*- and *Raf*-induced senescence, but not in mock cells. Sox2 regulates Atg10 expression and induces cellular senescence through autophagy phenomenon[41]. Upregulation of *Bmp2* and downregulation of *Smad6* were found in *Ras*-induced senescence in our previous study, and will be discussed in detail below. Alteration of these factors may play a role in both *Ras*- and *Raf*-induced senescence, but not in replicative senescence.

Although there are not so many genes, genes showing expression changes specifically in either *Ras*- or *Raf*-induced senescence also include interesting genes. *Wnt2* and *Hey1* were downregulated specifically in *Ras*-induced senescence, but not in *Raf*-induced senescence or mock cells (Figure 6). *Wnt2* is repressed in *Ras*-induced senescence, and the knockdown of *Wnt2* increases amount of SAHF and HIRA foci[42]. Targeting *Maml1* in melanoma cells was reported to suppress the downstream transcriptional repressor *Hey1*, resulting in senescence differentiation of melanoma cells, and increased melanin production[43].

Cd40 was upregulated, and *Mcam* and *Nfia* were downregulated specifically in *Raf*-induced senescence, but not in *Ras*-induced senescence or mock cells (Figure 6). *Cd40* was upregulated in senescence by histone deacetylase inhibitors[44]. The knockdown of *Mcam* in human mesenchymal stromal cells caused positive SA-β-gal staining[45]. *Nfia* promoted proliferation of glioma cells, and knockdown of *Nfia* by shRNA inhibited their proliferation[46]. *Raf*-specific alteration of these genes may play a specific role in *Raf*-induced senescence.

Among the genes showing expression alteration commonly or specifically in *Ras*- and *Raf*-induced senescence, we focused on an increase of *Bmp2* and decrease of *Smad6*. These alterations were commonly observed in *Ras*- and *Raf*-induced senescence, but not

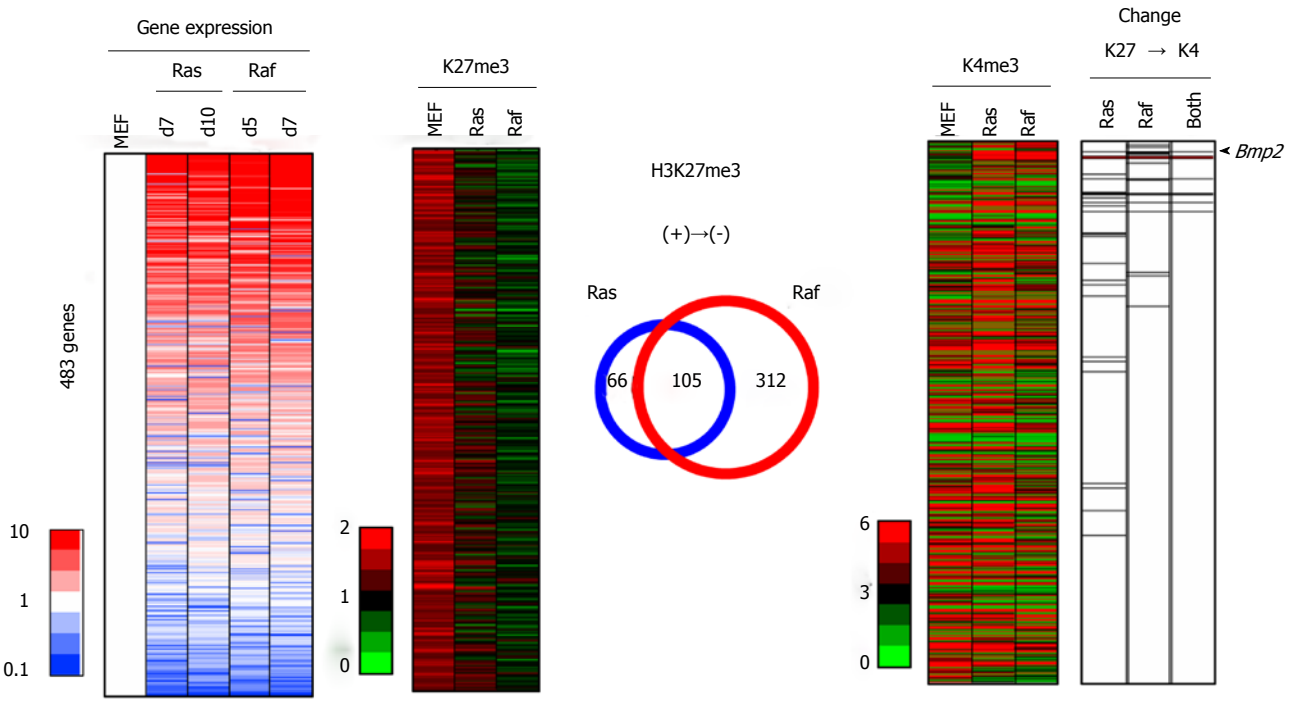

Figure 9 Integrated analysis of epigenetic and expression changes for genes losing H3K27me3. A total of 483 genes showed > 1.5 reads per 1000000 reads in MEF, but decreased to < 1.0 in both or either *Ras*- and *Raf*-induced senescence, and were sorted by the fold expression change between MEF and mean of RasG12V cells and RafV600E cells (left). Among these 483 genes losing H3K27me3 in senescence, 27 genes in *Ras*-induced senescence and 18 genes in *Raf*-induced senescence showed loss of H3K27me3 and gain of H3K4me3 (with increase from < 3.0 reads in MEF to > 3.5 reads in senescence) simultaneously, and 9 genes showed a simultaneous H3K27me3 loss and H3K4me3 gain in both *Ras*- and *Raf*-induced senescence (right). These genes showed a significant enrichment in upregulated genes among the 483 genes ($P = 1 \times 10^{-5}$ in *Ras*-induced senescence, $P = 2 \times 10^{-9}$ in *Raf*-induced senescence, and $P = 2 \times 10^{-8}$ in both senescence, Kolmogorov-Smirnov test), and included *Bmp2* (arrow head). Regarding the overlap of H3K27me3 alterations (center), 171 genes with H3K27me3 loss in Ras-induced senescence and 417 genes with H3K27me3 loss in *Raf*-induced senescence overlapped well (105 genes, $P < 1 \times 10^{-15}$, phi coefficient = 0.386).

in mock cells. In our previous study, the coordinated epigenetic regulation of these changes was found to be critical in *Ras*-induced senescence[22]. In this study, knockdown of *Bmp2* by shRNA and induction of *Smad6* in *Raf*-activated cells showed escape from senescence, indicating that increase of *Bmp2* and decrease of *Smad6* are also important in *Raf*-induced senescence as well as *Ras*-induced senescence. In colorectal cancer, disruption of Bmp2-Smad signaling has been suggested to be important. While the expression of BMP2 was observed in mature colonic epithelium, promoting differentiation and inhibiting proliferation, the expression of BMP2 was lost in adenoma of familial adenomatous polyposis[47]. In sporadic colorectal cancer, BMPR2, BMPR1A, and SMAD4 were frequently inactivated, correlating with loss of Smad1 phosphorylation[48]. The germline mutation of genes in BMP signaling causes Juvenile polyposis syndrome, a hereditary disease with increased risk of colorectal cancer[49,50]. Recently, we performed targeted exon sequencing analysis in colorectal tumors, and *BRAF*-mutation(+) high-methylation colorectal cancer showed the frequent mutation of genes in BMP signaling, *e.g.*, *BMPR2*, *BMP2*, and *SMAD4*[33]. Disruption of Bmp2-Smad signaling by mutation may play an important role in escaping from *Raf*-induced senescence and establish *Raf*-mutation(+) cancer.

The epigenetic alterations to regulate these upregulated and downregulated genes were mostly similar. Gain and loss of H3K4me3, and loss of H3K27me3 showed a significant overlap between *Ras*- and *Raf*-induced senescence. These epigenetic changes in *Bmp2* and *Smad6* promoter regions were commonly observed in *Ras*- and *Raf*-induced senescence. However, gain of H3K27me3 was quite different between *Ras*- and *Raf*-induced senescence on genome-wide scale. For *Smad6*, it was repressed by loss of H3K4me3 and gain of H3K27me3 in *Ras*-induced senescence, but by only loss of H3K4me3 without gain of H3K27me3 in *Raf*-induced senescence.

Although the mechanism to program epigenetic regulations is largely unknown, non-coding RNA might be involved[51,52]. PRC2 is known to be recruited to target genes in *trans* through an association with HOTAIR, a non-coding RNA at the *HOXC* locus[53]. Antisense non-coding RNA in the INK4 locus, ANRIL, binds to PRC1 and PRC2, and represses genes within INK4b/ARF/INK4a locus in *cis*, but ANRIL was downregulated when *Ras* was activated and these genes were upregulated[54,55]. It might be interesting to analyze whether PRC is recruited to the *Smad6* or *Bmp2* region by any non-coding RNAs in *cis* or *trans*, and the similarities and differences in epigenetic alterations in these gene regions during *Ras*- and *Raf*-induced senescence is caused by an expression

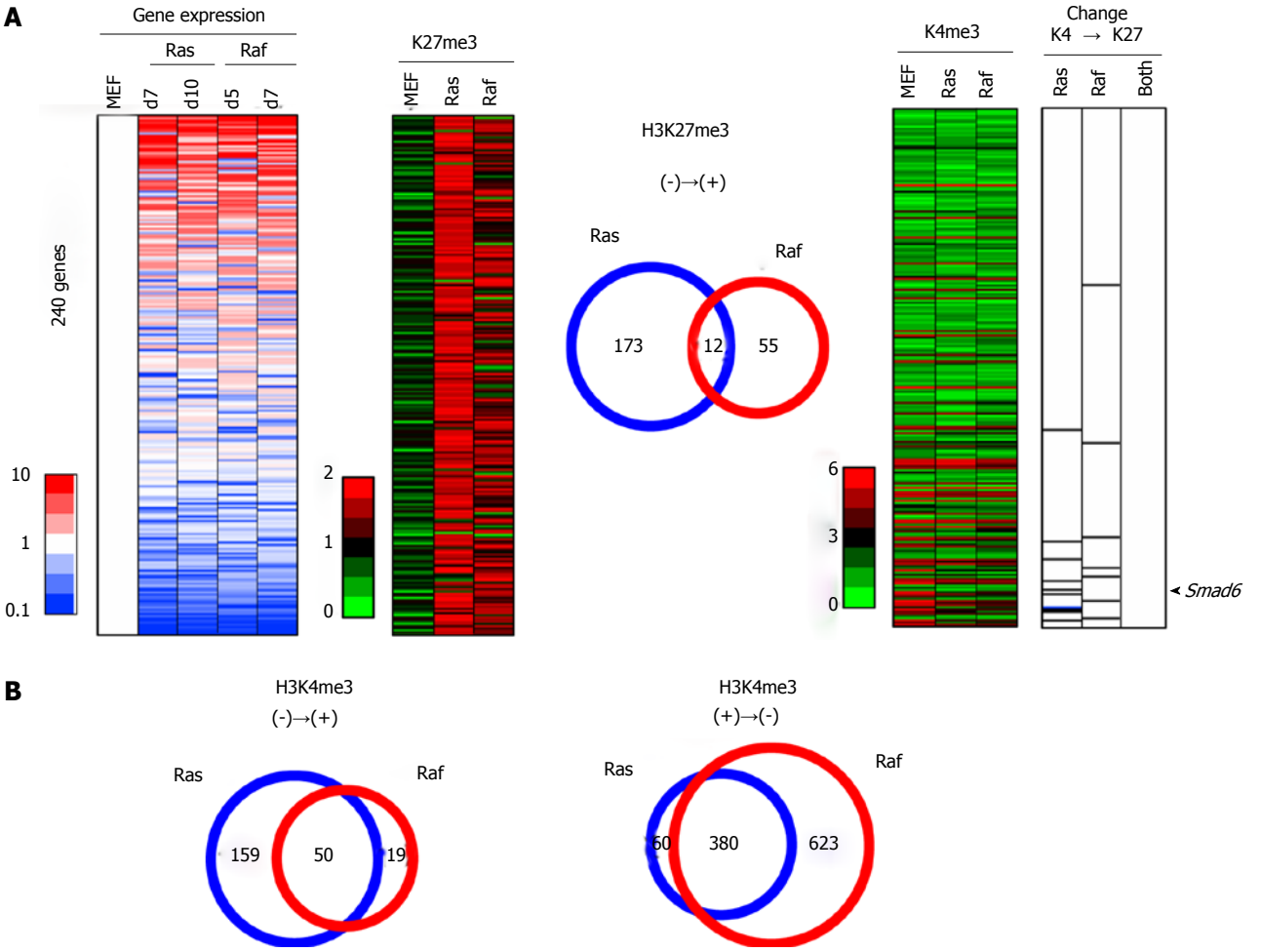

Figure 10 Integrated analysis of epigenetic and expression changes for genes acquiring H3K27me3. A: A total of 240 genes showed < 1.0 reads per 1000000 reads in MEF, but increased to > 1.5 in both or either of *Ras*- and *Raf*-induced senescence, and were sorted by the fold expression change between MEF and mean of RasG12V cells and RafV600E cells (left). Among these 240 genes acquiring de novo H3K27me3 in senescence, 10 genes in *Ras*-induced senescence and 7 genes in Raf-induced senescence showed a simultaneous gain of H3K27me3 and loss of H3K4me3 (right). These genes showed a significant enrichment in downregulated genes among the 240 genes ($P = 4 \times 10^{-6}$ in *Ras*-induced senescence, and $P = 0.02$ in *Raf*-induced senescence, Kolmogorov-Smirnov test). However, these 10 genes, *e.g.*, *Smad6* (arrow head), and 7 genes did not overlap at all. Regarding the overlap of H3K27me3 alterations (center), 185 genes with H3K27me3 gain in *Ras*-induced senescence and 67 genes with H3K27me3 gain in *Raf*-induced senescence showed limited overlap (12 genes only, phi coefficient = 0.103), and this overlap in H3K27me3 gain was markedly rare compared with the overlap in H3K27me3 loss (Figure 9) ($P < 1 \times 10^{-15}$, log linear analysis); B: Overlap of H3K4me3 alterations. Genes with H3K4me3 gain in *Ras*- and *Raf* induced senescence overlapped well (50 genes, $P < 1 \times 10^{-15}$, phi coefficient = 0.413) (left), and also genes with H3K4me3 loss in *Ras*- and *Raf*-induced senescence overlapped well (380 genes, $P < 1 \times 10^{-15}$, phi coefficient = 0.559) (right). The overlap in H3K27me3 gain (Figure 10A) was again markedly rare, compared with the overlap in H3K4me3 gain ($P = 2 \times 10^{-9}$, log linear analysis) or with that in H3K4me3 loss ($P < 1 \times 10^{-15}$, log linear analysis).

alteration of non-coding RNAs.

While the epigenetic regulation of the *Smad6* locus was somewhat different between *Ras*- and *Raf*-induced senescence, some other genes showing expression changes specifically in either of *Ras*- and *Raf*-induced senescence, were accompanied by different epigenomic alterations. *Nfia* was downregulated specifically in *Raf*-induced senescence, with H3K4me3 lost specifically in *Raf*-induced senescence. The difference in epigenetic alteration may cause difference in gene expression patterns, at least in part, and may result in difference in genesis for senescence.

In summary, while gene expression changes are mostly similar between *Ras*- and *Raf*-induced senescence, the upregulation of *Bmp2* and repression of *Smad6* were also important in *Raf*-induced senescence, and epigenetic alterations might be somewhat different, *e.g.,* in gain of H3K27me3 marks.

ACKNOWLEDGMENTS

The authors would like to thank Takanori Fujita, Kyoko Fujinaka, Hiroko Meguro and Kaori Shiina for technical assistance.

COMMENTS

Background

When an oncogene is activated, cells lead to cellular senescence, *i.e.*, irreversible growth arrest as a barrier against malignant transformation. In the authors previous studies, the authors performed a comprehensive analysis of aberrant DNA methylation in colorectal cancer, and reported three subtypes of

colorectal cancer with distinct DNA methylation epigenotypes. Different patterns of aberrant methylation accumulation significantly correlated with distinct oncogene mutations, suggesting that the accumulation of aberrant methylation might be a requested phenotype for oncogenic transformation by inactivation of critical factors for oncogene-induced senescence. To gain insight into critical gene inactivation in oncogene-mutation(+) cancer, the authors previously analyzed epigenomic and gene expression alterations in *Ras*-induced senescence in normal cells, and found a critical role of Bmp2-Smad signaling in *Ras*-induced senescence and its regulation by coordinated epigenetic alteration.

Research frontiers

The author aimed to investigate critical genes in *Raf*-induced senescence, and any difference between *Ras*- and *Raf*-induced senescence, to gain insight into critical gene inactivation in *Ras*-mutation(+) and *Raf*-mutation(+) colorectal cancer.

Innovations and breakthroughs

This study demonstrates that while some genes including those related to secreted factors showed expression changes specifically in *Ras*- or *Raf*-induced senescence, expression of many genes was commonly altered in *Ras*- and *Raf*-induced senescence. These changes include an increase of *Bmp2* and decrease of *Smad6*, and play a role in *Raf*-induced senescence as well as *Ras*-induced senescence. Epigenetic changes are also similar, but somewhat different, *e.g.,* gain of H3K27me3 in the *Smad6* promoter region.

Applications

The authors hypothesize that critical gene expression changes in oncogene-induced senescence should be disrupted in oncogene-mutation(+) cancer, to escape from growth arrest. DNA methylation and target exon sequencing are under analysis for colorectal cancer. An integrated analysis of these data will reveal different genesis of colorectal cancer with mutation of different oncogene.

Terminology

Comprehensive genomic and epigenomic data can stratify cancer into several subtypes. Colorectal cancer is stratified into *BRAF*-mutation(+) cancer, *KRAS*-mutation(+) cancer, and oncogene-mutation(-) cancer. These subgroups show different tumor morphologies, and accompany different genetic and epigenetic alterations, suggesting that these subgroups of cancer may arise through different tumorigenic mechanisms.

Peer-reivew

In this study, the authors examined the expression changes induced by oncogenic RAF. Previously, the authors have conducted similar study on oncogenic Ras.

REFERENCES

1 **Hayflick L**. The limited in vitro lifetime of human diploid cell strains. *Exp Cell Res* 1965; **37**: 614-636 [PMID: 14315085 DOI: 10.1016/0014-4827(65)90211-9]

2 **Serrano M**, Lin AW, McCurrach ME, Beach D, Lowe SW. Oncogenic ras provokes premature cell senescence associated with accumulation of p53 and p16INK4a. *Cell* 1997; **88**: 593-602 [PMID: 9054499 DOI: 10.1016/S0092-8674(00)81902-9]

3 **Kuilman T**, Michaloglou C, Mooi WJ, Peeper DS. The essence of senescence. *Genes Dev* 2010; **24**: 2463-2479 [PMID: 21078816 DOI: 10.1101/gad.1971610]

4 **Campisi J**. Senescent cells, tumor suppression, and organismal aging: good citizens, bad neighbors. *Cell* 2005; **120**: 513-522 [PMID: 15734683 DOI: 10.1016/j.cell.2005.02.003]

5 **Narita M**, Lowe SW. Senescence comes of age. *Nat Med* 2005; **11**: 920-922 [PMID: 16145569 DOI: 10.1038/nm0905-920]

6 **Prieur A**, Peeper DS. Cellular senescence in vivo: a barrier to tumorigenesis. *Curr Opin Cell Biol* 2008; **20**: 150-155 [PMID: 18353625 DOI: 10.1016/j.ceb.2008.01.007]

7 **Ivanov A**, Adams PD. A damage limitation exercise. *Nat Cell Biol* 2011; **13**: 193-195 [PMID: 21364567 DOI: 10.1038/ncb0311-193]

8 **Lowe SW**, Cepero E, Evan G. Intrinsic tumour suppression. *Nature* 2004; **432**: 307-315 [PMID: 15549092 DOI: 10.1038/nature03098]

9 **Ohtani N**, Hara E. Roles and mechanisms of cellular senescence in regulation of tissue homeostasis. *Cancer Sci* 2013; **104**: 525-530 [PMID: 23360516 DOI: 10.1111/cas.12118]

10 **Rodier F**, Campisi J. Four faces of cellular senescence. *J Cell Biol* 2011; **192**: 547-556 [PMID: 21321098 DOI: 10.1083/jcb.201009094]

11 **Courtois-Cox S**, Jones SL, Cichowski K. Many roads lead to oncogene-induced senescence. *Oncogene* 2008; **27**: 2801-2809 [PMID: 18193093 DOI: 10.1038/sj.onc.1210950]

12 **Lee AC**, Fenster BE, Ito H, Takeda K, Bae NS, Hirai T, Yu ZX, Ferrans VJ, Howard BH, Finkel T. Ras proteins induce senescence by altering the intracellular levels of reactive oxygen species. *J Biol Chem* 1999; **274**: 7936-7940 [PMID: 10075689 DOI: 10.1074/jbc.274.12.7936]

13 **Bartkova J**, Rezaei N, Liontos M, Karakaidos P, Kletsas D, Issaeva N, Vassiliou LV, Kolettas E, Niforou K, Zoumpourlis VC, Takaoka M, Nakagawa H, Tort F, Fugger K, Johansson F, Sehested M, Andersen CL, Dyrskjot L, Ørntoft T, Lukas J, Kittas C, Helleday T, Halazonetis TD, Bartek J, Gorgoulis VG. Oncogene-induced senescence is part of the tumorigenesis barrier imposed by DNA damage checkpoints. *Nature* 2006; **444**: 633-637 [PMID: 17136093 DOI: 10.1038/nature05268]

14 **Di Micco R**, Fumagalli M, Cicalese A, Piccinin S, Gasparini P, Luise C, Schurra C, Garre' M, Nuciforo PG, Bensimon A, Maestro R, Pelicci PG, d'Adda di Fagagna F. Oncogene-induced senescence is a DNA damage response triggered by DNA hyper-replication. *Nature* 2006; **444**: 638-642 [PMID: 17136094 DOI: 10.1038/nature05327]

15 **Sharpless NE**, DePinho RA. Cancer: crime and punishment. *Nature* 2005; **436**: 636-637 [PMID: 16079829 DOI: 10.1038/436636a]

16 **Gil J**, Peters G. Regulation of the INK4b-ARF-INK4a tumour suppressor locus: all for one or one for all. *Nat Rev Mol Cell Biol* 2006; **7**: 667-677 [PMID: 16921403 DOI: 10.1038/nrm1987]

17 **Rodier F**, Coppé JP, Patil CK, Hoeijmakers WA, Muñoz DP, Raza SR, Freund A, Campeau E, Davalos AR, Campisi J. Persistent DNA damage signalling triggers senescence-associated inflammatory cytokine secretion. *Nat Cell Biol* 2009; **11**: 973-979 [PMID: 19597488 DOI: 10.1038/ncb1909]

18 **Coppé JP**, Desprez PY, Krtolica A, Campisi J. The senescence-associated secretory phenotype: the dark side of tumor suppression. *Annu Rev Pathol* 2010; **5**: 99-118 [PMID: 20078217 DOI: 10.1146/annurev-pathol-121808-102144]

19 **Kuilman T**, Michaloglou C, Vredeveld LC, Douma S, van Doorn R, Desmet CJ, Aarden LA, Mooi WJ, Peeper DS. Oncogene-induced senescence relayed by an interleukin-dependent inflammatory network. *Cell* 2008; **133**: 1019-1031 [PMID: 18555778 DOI: 10.1016/j.cell.2008.03.039]

20 **Acosta JC**, O'Loghlen A, Banito A, Guijarro MV, Augert A, Raguz S, Fumagalli M, Da Costa M, Brown C, Popov N, Takatsu Y, Melamed J, d'Adda di Fagagna F, Bernard D, Hernando E, Gil J. Chemokine signaling via the CXCR2 receptor reinforces senescence. *Cell* 2008; **133**: 1006-1018 [PMID: 18555777 DOI: 10.1016/j.cell.2008.03.038]

21 **Chien Y**, Scuoppo C, Wang X, Fang X, Balgley B, Bolden JE, Premsrirut P, Luo W, Chicas A, Lee CS, Kogan SC, Lowe SW. Control of the senescence-associated secretory phenotype by NF-κB promotes senescence and enhances chemosensitivity. *Genes Dev* 2011; **25**: 2125-2136 [PMID: 21979375 DOI: 10.1101/gad.17276711]

22 **Kaneda A**, Fujita T, Anai M, Yamamoto S, Nagae G, Morikawa M, Tsuji S, Oshima M, Miyazono K, Aburatani H. Activation of Bmp2-Smad1 signal and its regulation by coordinated alteration of H3K27 trimethylation in Ras-induced senescence. *PLoS Genet* 2011; **7**: e1002359 [PMID: 22072987 DOI: 10.1371/journal.pgen.1002359]

23 **Kaneda A**, Wang CJ, Cheong R, Timp W, Onyango P, Wen B, Iacobuzio-Donahue CA, Ohlsson R, Andraos R, Pearson MA, Sharov AA, Longo DL, Ko MS, Levchenko A, Feinberg AP. Enhanced sensitivity to IGF-II signaling links loss of imprinting of

IGF2 to increased cell proliferation and tumor risk. *Proc Natl Acad Sci USA* 2007; **104**: 20926-20931 [PMID: 18087038 DOI: 10.1073/pnas.0710359105]

24 **Coppé JP**, Patil CK, Rodier F, Sun Y, Muñoz DP, Goldstein J, Nelson PS, Desprez PY, Campisi J. Senescence-associated secretory phenotypes reveal cell-nonautonomous functions of oncogenic RAS and the p53 tumor suppressor. *PLoS Biol* 2008; **6**: 2853-2868 [PMID: 19053174 DOI: 10.1371/journal.pbio.0060301]

25 **Narita M**, Nũnez S, Heard E, Narita M, Lin AW, Hearn SA, Spector DL, Hannon GJ, Lowe SW. Rb-mediated heterochromatin formation and silencing of E2F target genes during cellular senescence. *Cell* 2003; **113**: 703-716 [PMID: 12809602 DOI: 10.1016/S0092-8674(03)00401-X]

26 **Parrinello S**, Samper E, Krtolica A, Goldstein J, Melov S, Campisi J. Oxygen sensitivity severely limits the replicative lifespan of murine fibroblasts. *Nat Cell Biol* 2003; **5**: 741-747 [PMID: 12855956 DOI: 10.1038/ncb1024]

27 **Jacobs JJ**, Kieboom K, Marino S, DePinho RA, van Lohuizen M. The oncogene and Polycomb-group gene bmi-1 regulates cell proliferation and senescence through the ink4a locus. *Nature* 1999; **397**: 164-168 [PMID: 9923679 DOI: 10.1038/16476]

28 **Bracken AP**, Kleine-Kohlbrecher D, Dietrich N, Pasini D, Gargiulo G, Beekman C, Theilgaard-Mönch K, Minucci S, Porse BT, Marine JC, Hansen KH, Helin K. The Polycomb group proteins bind throughout the INK4A-ARF locus and are disassociated in senescent cells. *Genes Dev* 2007; **21**: 525-530 [PMID: 17344414 DOI: 10.1101/gad.415507]

29 **Kotake Y**, Cao R, Viatour P, Sage J, Zhang Y, Xiong Y. pRB family proteins are required for H3K27 trimethylation and Polycomb repression complexes binding to and silencing p16INK4alpha tumor suppressor gene. *Genes Dev* 2007; **21**: 49-54 [PMID: 17210787 DOI: 10.1101/gad.1499407]

30 **Agger K**, Cloos PA, Rudkjaer L, Williams K, Andersen G, Christensen J, Helin K. The H3K27me3 demethylase JMJD3 contributes to the activation of the INK4A-ARF locus in response to oncogene- and stress-induced senescence. *Genes Dev* 2009; **23**: 1171-1176 [PMID: 19451217 DOI: 10.1101/gad.510809]

31 **Barradas M**, Anderton E, Acosta JC, Li S, Banito A, Rodriguez-Niedenführ M, Maertens G, Banck M, Zhou MM, Walsh MJ, Peters G, Gil J. Histone demethylase JMJD3 contributes to epigenetic control of INK4a/ARF by oncogenic RAS. *Genes Dev* 2009; **23**: 1177-1182 [PMID: 19451218 DOI: 10.1101/gad.511109]

32 **Dimri GP**, Lee X, Basile G, Acosta M, Scott G, Roskelley C, Medrano EE, Linskens M, Rubelj I, Pereira-Smith O. A biomarker that identifies senescent human cells in culture and in aging skin in vivo. *Proc Natl Acad Sci USA* 1995; **92**: 9363-9367 [PMID: 7568133]

33 **Sakai E,** Fukuyo M, Ohata K, Matsusaka K, Doi N, Mano Y, Takane K, Abe H, Yagi K, Matsuhashi N, Fukushima J, Fukayama M, Akagi K, Aburatani H, Nakajima A, Kaneda A. Genetic and epigenetic aberrations occurring in colorectal tumors associated with serrated pathway. *Int J Cancer* 2016; **138**: 1634-1644 [PMID: 26510091 DOI: 10.1002/ijc.29903]

34 **Narita M**, Narita M, Krizhanovsky V, Nuñez S, Chicas A, Hearn SA, Myers MP, Lowe SW. A novel role for high-mobility group a proteins in cellular senescence and heterochromatin formation. *Cell* 2006; **126**: 503-514 [PMID: 16901784 DOI: 10.1016/j.cell.2006.05.052]

35 **Jeanblanc M**, Ragu S, Gey C, Contrepois K, Courbeyrette R, Thuret JY, Mann C. Parallel pathways in RAF-induced senescence and conditions for its reversion. *Oncogene* 2012; **31**: 3072-3085 [PMID: 22020327 DOI: 10.1038/onc.2011.481]

36 **Collado M**, Gil J, Efeyan A, Guerra C, Schuhmacher AJ, Barradas M, Benguría A, Zaballos A, Flores JM, Barbacid M, Beach D, Serrano M. Tumour biology: senescence in premalignant tumours. *Nature* 2005; **436**: 642 [PMID: 16079833]

37 **Zhu J**, Woods D, McMahon M, Bishop JM. Senescence of human fibroblasts induced by oncogenic Raf. *Genes Dev* 1998; **12**: 2997-3007 [PMID: 9765202 DOI: 10.1101/gad.12.19.2997]

38 **Michaloglou C**, Vredeveld LC, Soengas MS, Denoyelle C, Kuilman T, van der Horst CM, Majoor DM, Shay JW, Mooi WJ, Peeper DS. BRAFE600-associated senescence-like cell cycle arrest of human naevi. *Nature* 2005; **436**: 720-724 [PMID: 16079850 DOI: 10.1038/nature03890]

39 **Fernández-Barral A**, Orgaz JL, Baquero P, Ali Z, Moreno A, Tiana M, Gómez V, Riveiro-Falkenbach E, Cañadas C, Zazo S, Bertolotto C, Davidson I, Rodríguez-Peralto JL, Palmero I, Rojo F, Jensen LD, del Peso L, Jiménez B. Regulatory and functional connection of microphthalmia-associated transcription factor and anti-metastatic pigment epithelium derived factor in melanoma. *Neoplasia* 2014; **16**: 529-542 [PMID: 25030625 DOI: 10.1016/j.neo.2014.06.001]

40 **Varecza Z**, Kvell K, Talabér G, Miskei G, Csongei V, Bartis D, Anderson G, Jenkinson EJ, Pongracz JE. Multiple suppression pathways of canonical Wnt signalling control thymic epithelial senescence. *Mech Ageing Dev* 2011; **132**: 249-256 [PMID: 21549744 DOI: 10.1016/j.mad.2011.04.007]

41 **Cho YY**, Kim DJ, Lee HS, Jeong CH, Cho EJ, Kim MO, Byun S, Lee KY, Yao K, Carper A, Langfald A, Bode AM, Dong Z. Autophagy and cellular senescence mediated by Sox2 suppress malignancy of cancer cells. *PLoS One* 2013; **8**: e57172 [PMID: 23451179 DOI: 10.1371/journal.pone.0057172]

42 **Kuilman T**, Peeper DS. Senescence-messaging secretome: SMS-ing cellular stress. *Nat Rev Cancer* 2009; **9**: 81-94 [PMID: 19132009 DOI: 10.1038/nrc2560]

43 **Kang S**, Xie J, Miao J, Li R, Liao W, Luo R. A knockdown of Maml1 that results in melanoma cell senescence promotes an innate and adaptive immune response. *Cancer Immunol Immunother* 2013; **62**: 183-190 [PMID: 22864395 DOI: 10.1007/s00262-012-1318-1]

44 **Gregorie CJ**, Wiesen JL, Magner WJ, Lin AW, Tomasi TB. Restoration of immune response gene induction in trophoblast tumor cells associated with cellular senescence. *J Reprod Immunol* 2009; **81**: 25-33 [PMID: 19493573 DOI: 10.1016/j.jri.2009.02.009]

45 **Stopp S**, Bornhäuser M, Ugarte F, Wobus M, Kuhn M, Brenner S, Thieme S. Expression of the melanoma cell adhesion molecule in human mesenchymal stromal cells regulates proliferation, differentiation, and maintenance of hematopoietic stem and progenitor cells. *Haematologica* 2013; **98**: 505-513 [PMID: 22801967 DOI: 10.3324/haematol.2012.065201]

46 **Lee JS**, Xiao J, Patel P, Schade J, Wang J, Deneen B, Erdreich-Epstein A, Song HR. A novel tumor-promoting role for nuclear factor IA in glioblastomas is mediated through negative regulation of p53, p21, and PAI1. *Neuro Oncol* 2014; **16**: 191-203 [PMID: 24305710 DOI: 10.1093/neuonc/not167]

47 **Hardwick JC**, Van Den Brink GR, Bleuming SA, Ballester I, Van Den Brande JM, Keller JJ, Offerhaus GJ, Van Deventer SJ, Peppelenbosch MP. Bone morphogenetic protein 2 is expressed by, and acts upon, mature epithelial cells in the colon. *Gastroenterology* 2004; **126**: 111-121 [PMID: 14699493 DOI: 10.1053/j.gastro.2003.10.067]

48 **Kodach LL**, Wiercinska E, de Miranda NF, Bleuming SA, Musler AR, Peppelenbosch MP, Dekker E, van den Brink GR, van Noesel CJ, Morreau H, Hommes DW, Ten Dijke P, Offerhaus GJ, Hardwick JC. The bone morphogenetic protein pathway is inactivated in the majority of sporadic colorectal cancers. *Gastroenterology* 2008; **134**: 1332-1341 [PMID: 18471510]

49 **Haramis AP**, Begthel H, van den Born M, van Es J, Jonkheer S, Offerhaus GJ, Clevers H. De novo crypt formation and juvenile polyposis on BMP inhibition in mouse intestine. *Science* 2004; **303**: 1684-1686 [PMID: 15017003 DOI: 10.1126/science.1093587]

50 **Howe JR**, Bair JL, Sayed MG, Anderson ME, Mitros FA, Petersen GM, Velculescu VE, Traverso G, Vogelstein B. Germline mutations of the gene encoding bone morphogenetic protein receptor 1A in juvenile polyposis. *Nat Genet* 2001; **28**: 184-187 [PMID: 11381269 DOI: 10.1038/88919]

51 **Zhao J**, Sun BK, Erwin JA, Song JJ, Lee JT. Polycomb proteins targeted by a short repeat RNA to the mouse X chromosome. *Science* 2008; **322**: 750-756 [PMID: 18974356]

52 **Hirota K**, Miyoshi T, Kugou K, Hoffman CS, Shibata T, Ohta K. Stepwise chromatin remodelling by a cascade of transcription initiation of non-coding RNAs. *Nature* 2008; **456**: 130-134 [PMID:

18820678 DOI: 10.1038/nature07348]

53 **Rinn JL**, Kertesz M, Wang JK, Squazzo SL, Xu X, Brugmann SA, Goodnough LH, Helms JA, Farnham PJ, Segal E, Chang HY. Functional demarcation of active and silent chromatin domains in human HOX loci by noncoding RNAs. *Cell* 2007; **129**: 1311-1323 [PMID: 17604720 DOI: 10.1016/j.cell.2007.05.022]

54 **Yap KL**, Li S, Muñoz-Cabello AM, Raguz S, Zeng L, Mujtaba S, Gil J, Walsh MJ, Zhou MM. Molecular interplay of the noncoding RNA ANRIL and methylated histone H3 lysine 27 by polycomb CBX7 in transcriptional silencing of INK4a. *Mol Cell* 2010; **38**: 662-674 [PMID: 20541999 DOI: 10.1016/j.molcel.2010.03.021]

55 **Kotake Y**, Nakagawa T, Kitagawa K, Suzuki S, Liu N, Kitagawa M, Xiong Y. Long non-coding RNA ANRIL is required for the PRC2 recruitment to and silencing of p15(INK4B) tumor suppressor gene. *Oncogene* 2011; **30**: 1956-1962 [PMID: 21151178 DOI: 10.1038/onc.2010.568]

P- Reviewer: Bai G, Wang Y
S- Editor: Qi Y **L- Editor**: A **E- Editor**: Jiao XK

Published by **Baishideng Publishing Group Inc**
8226 Regency Drive, Pleasanton, CA 94588, USA
Telephone: +1-925-223-8242
Fax: +1-925-223-8243
E-mail: bpgoffice@wjgnet.com
Help Desk: http://www.wjgnet.com/esps/helpdesk.aspx
http://www.wjgnet.com